Structure and proteolytic susceptibility of the inhibitory C-terminal tail of cardiac troponin I

Zabed Mahmud[1§], Somaya Zahran[4§], Philip B. Liu[1], Bela Reiz[5], Brandon Y.H Chan[2,3], Andrej Roczkowsky[2,3], Christian-Scott E. McCartney[6], Peter L. Davies[6], Liang Li[5], Richard Schulz[2,3], Peter M. Hwang[1, 4*]

1. Department of Biochemistry, University of Alberta, Edmonton, AB, T6G 2R3, Canada
2. Department of Pediatrics, University of Alberta, Edmonton, AB, T6G 1C9, Canada
3. Department of Pharmacology, University of Alberta, Edmonton, AB, T6G 2H7, Canada
4. Department of Medicine, University of Alberta, Edmonton, AB, T6G 2R3, Canada
5. Department of Chemistry, University of Alberta, Edmonton, AB, T6G 2G2, Canada
6. Department of Biomedical and Molecular Sciences, Queen's University, Kingston, ON, K7L 3N6, Canada

[§] Zabed Mahmud and Somaya Zahran contributed equally to this work

[*]To whom correspondence should be addressed: Dr. Peter M. Hwang, Departments of Medicine and Biochemistry, 3-08 Medical Sciences Building, University of Alberta, Edmonton, AB, Canada, T6G 2H7. Email: phwang1@ualberta.ca

Highlights:

1. The disordered C-terminal tail of cardiac troponin I (residues 135-209) plays an essential role, alternating between actin and cardiac troponin C to control the cardiac cycle
2. The C-terminal tail becomes partially structured upon binding actin
3. Both N- and C-terminal tails are susceptible to proteolysis by intracellular proteases MMP-2 and calpain-2
4. Both MMP-2 and calpain-2 cleave the critical switch region of cardiac troponin I, though it is protected when bound to actin or cardiac troponin C

Abstract

Background

Cardiac troponin I (cTnI) has two flexible tails that control the cardiac cycle. The C-terminal tail, $cTnI_{135-209}$, binds actin to shut off cardiac muscle contraction, whereas the competing calcium-dependent binding of the switch region, $cTnI_{146-158}$, by cardiac troponin C (cTnC) triggers contraction. The N-terminal tail, $cTnI_{1-37}$, regulates the calcium affinity of cTnC. cTnI is known to be susceptible to proteolytic cleavage by matrix metalloproteinase-2 (MMP-2) and calpain, two intracellular proteases implicated in ischemia-reperfusion injury.

Methods

Soluble fragments of cTnI containing its N- and C-terminal tails, $cTnI_{1-77}$ and $cTnI_{135-209}$, were highly expressed and purified from *E. coli*. We performed *in vitro* proteolysis studies of both constructs using liquid chromatography-mass spectrometry (LC-MS) and solution NMR studies of the C-terminal tail.

Results

$cTnI_{135-209}$ is intrinsically disordered, though it contains three regions with helical propensity (including the switch region) that acquire more structure upon actin binding. We identified three precise MMP-2 cleavage sites at cTnI P17-I18, A156-L157, and G199-M200. In contrast, calpain-2 has numerous cleavage sites throughout Y25-T30 and A152-A160. The critical cTnI switch region is targeted by both proteases.

Conclusions

Both N-terminal and C-terminal tails of cTnI are susceptible to cleavage by MMP-2 and calpain-2. Binding to cTnC or actin confers some protection to proteolysis, which can be understood in terms of their interactions as probed by NMR studies.

General Significance

cTnI is an important marker of intracellular proteolysis in cardiomyocytes, given its many protease-specific cut sites, high natural abundance, indispensable functional role, and clinical use as gold standard biomarker of myocardial injury.

Keywords

Nuclear magnetic resonance (NMR) spectroscopy, mass spectrometry, intrinsically disordered protein, myocardial infarction, ischemia-reperfusion injury, myocardial stunning, matrix metalloproteinase-2, calpain

Introduction

The cardiac troponin complex (cTn) links cyclic Ca^{2+} fluctuations to cardiac muscle contraction and relaxation **[1, 2]**. It is comprised of three subunits **[3]**: cTnC binds calcium; cTnT anchors the complex to tropomyosin; and cTnI is the inhibitory subunit (**Figure 1)**. Cardiac troponin I (cTnI) has two flexible tails that are critical to its function. The N-terminal tail, $cTnI_{1\text{-}38}$, interacts with the regulatory domain of cTnC (cNTnC) to enhance its calcium affinity. This effect is attenuated by phosphorylation of cTnI Ser22/Ser23 **[4]**, the primary post-translational modification regulating the calcium sensitivity of cardiac muscle contraction in humans **[5]**.

The C-terminal tail, $cTnI_{135\text{-}209}$, binds actin to anchor the troponin-tropomyosin complex to a "blocked" position that prevents actin-myosin cross-bridging during diastole (the ventricular relaxation phase of the cardiac cycle). During systole (the ventricular contraction phase), cNTnC binds the cTnI switch region, $cTnI_{146\text{-}158}$, in a calcium-dependent manner, to release the inhibitory effect of $cTnI_{135\text{-}209}$. Thus, the $cTnI_{135\text{-}209}$ C-terminal tail cycles back and forth between actin and cTnC during diastole and systole, respectively, driving the cardiac cycle. The interactions between cTnI and cTnC have been well established by X-ray crystallography and NMR spectroscopy **[6-8]**, but very little is known about the interaction between cTnI and actin.

The N-terminal and C-terminal tails of cTnI are flexible, solvent-exposed, and susceptible to post-translational modifications like proteolysis **[9, 10]**. Western blot analysis of serum cTnI in myocardial infarction patients demonstrates multiple cut sites within the cTnI N- and C-terminal tails **[11]**. In animal models, proteolytic digestion of cTnI has been demonstrated to occur in myocardial ischemia-reperfusion injury **[12-14]**. Two major mechanisms are known to contribute to ischemia-reperfusion injury: generation of excess reactive oxygen-nitrogen species **[15, 16]** and calcium overload **[17, 18]**. Both processes activate downstream proteases that can compromise structural integrity and promote cell death.

Matrix metalloproteinases (MMPs) were originally identified as extracellular proteases but were subsequently found to localize to intracellular compartments as well **[14, 19]**, with matrix metalloproteinase-2 (MMP-2) being the predominant isoform in cardiomyocytes. MMPs are synthesized as inactive zymogens, with an inhibitory cysteine residue in the pro-peptide domain complexing the catalytic zinc ion. MMPs are activated by proteolytic removal of the pro-peptide domain or by chemical modification of the inhibitory cysteine sulfhydryl group, as occurs when reactive oxygen-nitrogen species, particularly peroxynitrite **[20]**, are generated during ischemia-reperfusion injury **[21-23]**.

Calpains are a family of calcium-dependent cysteine proteases that are involved in cytoskeletal remodeling, signal transduction, and cell death **[24, 25]**. Calpain-1 (μ-calpain) and calpain-2 (m-calpain) are ubiquitously expressed and are activated by elevated intracellular Ca^{2+}

concentrations **[17, 18, 26-28]**. These calpains have nearly indistinguishable substrate specificities **[29, 30]** but differ in the concentration of calcium required for activation.

Both MMP-2 and calpain have been shown to cleave cTnI in animal models of ischemia-reperfusion injury **[14, 31]**. Small molecule inhibition of MMP-2 **[14, 32]** or calpain **[33-35]** has been shown to attenuate ischemia-reperfusion injury in animal models.

The structured core of cTnI (residues 39-134) is known to be relatively resistant to proteolytic digestion **[36]**. Moreover, since full-length cTnI misfolds and aggregates on its own, we generated two soluble fragments of cTnI containing its flexible protease-susceptible N- and C-terminal tails, $cTnI_{1-77}$ and $cTnI_{135-209}$, respectively. Using purified proteins and mass spectrometry, we have mapped out the precise cTnI cleavage sites for MMP-2 and calpain-2. Since cTnI interacts primarily with cTnC and actin *in vivo*, we also examine its proteolysis in the presence of these binding partners.

Given the extensive biophysical characterization of the troponin complex over the past six decades, it is possible to understand the proteolytic susceptibility of cTnI in terms of its structure. However, relatively little is known about the structure of the critical C-terminal tail bound to actin, because the intrinsic disorder of the tail, combined with the filamentous nature of actin, is difficult for any one biophysical technique to tackle comprehensively. In the current study, we use solution NMR spectroscopy to probe the structure of the C-terminal $cTnI_{135-209}$ tail without actin and in the presence of actin maintained in a monomeric form by its complex with DNase I (so that it can be studied by solution NMR).

Materials and methods

Protein expression and purification

Soluble recombinant human cTnI proteins, $cTnI_{1-77}$ and $cTnI_{135-209,}$ were expressed in *Escherichia coli* and purified as described previously **[37, 38]**. Briefly, both recombinant proteins were expressed as fusions to the β-barrel membrane protein, PagP. This causes the fusion protein to accumulate in insoluble inclusion bodies, which can be harvested by centrifugation, solubilized in 6 M guanidine-HCl, and then purified by nickel affinity chromatography. $cTnI_{1-77}$ was separated from PagP via cyanogen bromide cleavage in 0.1 M HCl **[37, 39]**, while $cTnI_{135-209}$ was separated using nickel ion-catalyzed cleavage **[38]**. $cTnI_{135-209}$ was produced with ^{15}N- and/or ^{13}C-isotope enrichment for solution NMR studies.

NMR Spectroscopy

All NMR data used in this study were generated at 30°C using a Varian Inova 500 MHz spectrometer equipped with a triple resonance probe and pulsed field gradients. NMR samples contained 500 µl of aqueous NMR buffer consisting of 10 mM imidazole, 0.5 mM 2,2-dimethyl-2-silapentane-5-sulfonate-d6 sodium salt (d_6-DSS), and 0.01 % NaN_3 in 90% H_2O, 10% D_2O or 100 % D_2O at pH 6.8. Three-dimensional HNCACB and CBCA(CO)NH experiments were carried out to obtain backbone ^{1}H, ^{15}N, ^{13}C chemical shift assignments for a sample of 2.8 mg $cTnI_{135-209}$ dissolved in NMR buffer. In addition, both (H)C(CO)NH-TOCSY and H(C)(CO)NH-TOCSY experiments were conducted to obtain side-chain ^{1}H and ^{13}C chemical shift assignments. 3D ^{15}N-edited and ^{13}C-edited homonuclear ^{1}H-^{1}H NOESY experiments were also performed and analyzed to obtain NOE information. All two- and three-dimensional NMR data were processed using NMRPipe/NMRDraw software **[40]**. NMRViewJ **[41]** from One Moon Scientific (http://www.onemoonscientific.com/nmrviewj) was used to further visualize and analyse spectra. The δ2D program **[42]** (http://www-mvsoftware.ch.cam.ac.uk/) was used to quantitate secondary structure propensities (α-helix, β-strand and random coil) using backbone chemical shift assignments **[43]**.

Recombinant bovine cardiac muscle actin (>99% pure, Cat. # AD99-A) was purchased from Cytoskeleton, Inc (U.S.A). RNase-free and protease-free deoxyribonuclease I (DNase I) was purchased from Worthington Biochemical Corporation. Actin was maintained in a monomeric form through its tight binding to DNase I, thereby inhibiting polymerization **[44]**.

^{15}N-labeled $cTnI_{135-209}$ (1.1 mg) was dissolved in 500 µL NMR buffer with an additional 10 mM DTT. A baseline (^{1}H, ^{15}N)-HSQC spectrum was recorded of this sample. Next, 1 mg of actin was dissolved in 100 µL NMR buffer + 10 mM DTT, added to 1 mg DNase I, and then mixed with the 500 µL solution of ^{15}N-labeled $cTnI_{135-209}$. The (^{1}H, ^{15}N)-HSQC spectrum was repeated, and a comparison of peak intensities before and after addition of monomeric actin-DNase I was obtained, after correcting for dilution.

The mathematical equation for calculating error bars is as follows:

$$\Delta\left(\frac{I}{I_0}\right) = \frac{\sqrt{I^2 {N_0}^2 + {I_0}^2 N^2}}{{I_0}^2}$$

Here,

$$\Delta\left(\frac{I}{I_0}\right) = Estimated\ error\ in\ signal\ intensity\ ratio$$

$$I = Signal\ intensity\ in\ the\ presence\ of\ actin - DNase\ I$$

$$I_0 = Signal\ intensity\ before\ adding\ actin - DNase\ I$$

$$N = Noise\ level\ in\ the\ presence\ of\ actin - DNase\ I$$

$$N_0 = Noise\ level\ before\ adding\ actin - DNase\ I$$

SDS-PAGE analysis of *in vitro* proteolysis

Purified human recombinant MMP-2 (72 kDa) (200 µg/ml) was activated chemically by 1 mM of 4-aminophenylmercuric acetate (APMA) in activation buffer (100 mM Tris-HCl, 10 mM $CaCl_2$, pH 7.6), as previously described **[45]**. Recombinant rat calpain-2 was expressed and purified as previously described **[46]**. APMA-activated recombinant human MMP-2 was incubated with $cTnI_{1-77}$ (0.1 µg/ µl) or $cTnI_{135-209}$ (0.1 µg/ µl) in incubation buffer (50 mM Tris-HCl, 5 mM $CaCl_2$, 150 mM NaCl, pH 7.6) for 2 h at 37°C. Similarly, recombinant rat calpain-2 was also incubated with $cTnI_{1-77}$ (0.1 µg/ µl) or $cTnI_{135-209}$ (0.1 µg/ µl) in incubation buffer (50 mM Tris-HCl, 5 mM $CaCl_2$, 150 mM NaCl, 10 mM beta mercaptoethanol, 10 mM DTT, pH 7.6) for 2 h at 37 °C. Proteolytic assays were carried out with enzyme-to-substrate molar ratios ranging from 1:500 to 1:10000 and 1:250 to 1:5000 for MMP-2:cTnI and calpain-2:cTnI respectively. As controls, 2-[((1, 1'-Biphenyl)-4-ylsulfonyl)-(1-methylethoxy) amino]-N-hydroxyacetamide (ARP-100) and MDL-28170 inhibitors [Cayman Chemical, USA] were used to block MMP-2 and calpain-2 activity, respectively. The products of all proteolysis assays were separated by electrophoresis in 16% Tris-Tricine gels and visualized by Coomassie blue staining.

In an additional set of experiments, activated MMP-2 or calpain-2 were incubated with $cTnI_{1-77}$ or $cTnI_{135-209}$ in the presence or absence of cTnC or actin. cTnC binds to cTnI with a 1:1 stoichiometry, so 0.32 µg/µl cTnC was used, corresponding to a 1.5:1 cTnC:cTnI ratio (excess cTnC). For actin, a 1:1 stoichiometry was suspected (discussed further in the Results section), therefore actin was added at a concentration of 0.50 µg/µl, corresponding to a 1:1 molar ratio. The actin concentration was then serially diluted two-fold to yield molar ratios ranging from 1:1 to 0.0625:1. Note that under these conditions, actin is predominantly in the filamentous F-actin form, though at the lowest concentrations used, there would be a more significant proportion of monomeric G-actin **[47]**.

Mass spectrometric analysis of *in vitro* proteolysis

A cocktail of MMP-2 (1 ng/µL) with $cTnI_{1-77}$ (0.43 µg/µl) or MMP-2 (1 ng/µL) with $cTnI_{135-209}$ (0.44 µg/µl), each at 1:5000 molar ratio, was incubated at 37°C for a time course study from 0 min to 24 h. The same time course study was applied to calpain-2 (4 ng/µL) with $cTnI_{1-77}$ (0.43 µg/µl) and calpain-2 (4 ng/µL) with $cTnI_{135-209}$ (0.44 µg/µl), each incubated at 1:1000 molar ratio at 37 °C. Formic acid (1% v/v) was used to denature the proteins and stop the reaction, and the

samples were immediately flash frozen with liquid nitrogen. For protein molecular weight determination reverse phase high performance liquid chromatography followed by mass spectrometry (RP-HPLC-MS) was performed using an Agilent 1200 SL HPLC System with a Poroshell 300SB-C8, 5-micron particle size, 75x0.5mm column (Agilent Technologies, USA), with Opti-pak trap cartridge kit, 5µL BED, C8, thermostated at 60 °C or a Phenomenex Aeris 3.6um, WIDEPORE XB-C8, 200Å, 2.1x50 mm with guard column, thermostated at 50 °C.

For the Poroshell column a buffer gradient system composed 0.1% formic acid in water as mobile phase A and 0.1% formic acid in acetonitrile as mobile phase B was used. An aliquot of 5 µL of sample was loaded onto the column at a flow rate of 0.15 ml/min and an initial buffer composition of 95% mobile phase A and 5% mobile phase B. After injection, the column was washed using the initial loading conditions for 3 min to effectively remove salts. Elution of the proteins was done by using a linear gradient from 5% to 50% mobile phase B for 10 min, 50% to 95% mobile phase B for 2 min, 95% to 98% mobile phase B for 4 min and back to 5% mobile phase B for of 1 min.

For the Phenomenex Aeris column following gradient was used: the column was washed after loading of the sample using a 0.4 ml/min flow rate and 5% mobile phase B for 2 min to effectively remove salts. Elution of the proteins was done using a linear gradient from 5% to 65% mobile phase B for 8 min, 65% to 98% mobile phase B over a period of 2 minute, kept at 98% mobile phase B for 2 min and back to 5% mobile phase B for 1 min.

Mass spectra were acquired in positive mode of ionization using an Agilent 6220 Accurate-Mass TOF HPLC/MS system (Santa Clara, CA, USA) equipped with a dual sprayer electrospray ionization source with the second sprayer providing a reference mass solution. Mass correction was performed for every individual spectrum using peaks at m/z 121.0509 and 922.0098 from the reference solution. Mass spectrometric conditions were drying gas 10 L/min at 325 °C, nebulizer 20 psi, mass range 100-3000 Da, acquisition rate of ~1.03 spectra/sec, fragmentor 200 V, skimmer 65 V, capillary 3200 V, instrument state 4 GHz High Resolution. Data analysis was performed using the Agilent MassHunter Qualitative Analysis software package version B.03.01 SP3. From the masses, the proteolysis fragments from both recombinant proteins were determined by using the online bioinformatics tool FindPept from the ExPASy server, **[48]** (http://web.expasy.org/findpept/). SequenceEditor (Build 5.65) from Bruker Daltonics Biotools 3.2 SR3 (https://www.bruker.com/service/support-upgrades/software-downloads/mass-spectrometry.html) was also used to analyse the peptide masses.

Results

Structure of free $cTnI_{135-209}$ by NMR spectroscopy

The ^{1}H-^{15}N HSQC spectrum of $cTnI_{135-209}$ in solution (see Figure 3A below) shows narrow and intense peaks with poor chemical shift dispersion, suggestive of an intrinsically disordered region. Some peaks are weak due to rapid backbone amide-solvent exchange, becoming more visible at more acidic pH due to the slowing of base-catalyzed solvent exchange, especially peaks corresponding to inhibitory region residues, 135-147. Near-complete chemical shift assignments of backbone and side chain resonances were obtained (and deposited in the Biological Magnetic Resonance Bank, **BMRB# 27476**).

Secondary structure analysis showed predominantly random coil structure, using the chemical shift analysis program δ2D, which determines the percentage of secondary structure based on HN, N, Hα, Cα, CO, and Cβ chemical shifts on a per residue basis. cTnI residues 150-159 are known to form an alpha-helix when the switch region binds cNTnC, and δ2D indicates that this region has the highest helical propensity (up to 50%) in $cTnI_{135-209}$ in the absence of cTnC (**Figure 2A**). Some helical character extends beyond the switch region out to residue 172, though this is not observed in X-ray or NMR structures **[6, 8]**. Slight helical propensity is also observed from residues 189 to 202 (though only up to ~10%). There is no significant β-sheet propensity anywhere in the $cTnI_{135-209}$ sequence.

Regions with helical propensity indicated by δ2D also had corroborating NOEs obtained from ^{13}C- and ^{15}N-edited NOESY-HSQC experiments. **Figure 2B** shows medium range $d_{\alpha\beta}$ (*i, i + 3*) NOEs that correspond to the helical regions identified by chemical shift analysis. The strongest helical NOEs were observed in the switch region, as shown in **Figure 2C**. The NOE pattern confirms nascent helix formation in residues 149-159, 164-172 and 187-197.

Our analysis of the cardiac troponin I C-terminal region is consistent with that of Blumenschein et al. **[49]**, who documented primarily disordered random coil in the corresponding region in fast skeletal troponin I. However, that study did not include an analysis of the helical switch region (unobservable due to the high molecular weight of the fast skeletal troponin complex), nor did it consider nascent helical structure via ^{1}H-^{1}H NOEs or backbone chemical shifts. In contrast to the Blumenschein study, Murakami et al. **[50]** describe a "mobile domain" in the C-terminal region of fast skeletal troponin I, made up of a small anti-parallel β-sheet extending from residues V143 to L154 (corresponding to V175 to N184 in cardiac troponin I, though according to sequence alignment, D153-L154 in fast skeletal troponin I are deleted in the cardiac isoform, precluding formation of a similar anti-parallel β-sheet in cTnI), packed against a helix extending from V157 to K167 (V187 to L197 in cTnI). It is important to note that the backbone chemical shifts obtained by Murakami agree with those obtained by Blumenschein, but these are not supportive of a rigid mobile domain structure. Thus, the "mobile domain" of Murakami et al. could be at most a transiently structured domain, which the authors support by the presence of many weak long range NOEs. In this regard, we note that our chemical shift and

NOE data are in agreement with Murakami et al. with respect to the presence of nascent helical structure in residues cTnI 164-172 and 187-197. However, there is no evidence of β-sheet formation in our construct, either by chemical shift or NOE analysis. As well, Murakami et al. noted the presence of an additional C-terminal helix that we do not observe in our construct, likely because of sequence differences between the fast skeletal and cardiac isoforms of troponin I.

Partial structuring of $cTnI_{135-209}$ in the presence of monomeric actin-DNase I

Many intrinsically disordered segments of proteins acquire structure upon binding to a protein partner. However, we previously found that $cTnI_{1-37}$ does not acquire any rigid secondary structure upon binding to the cNTnC domain through predominantly electrostatic interactions **[39]**. In contrast, hydrophobic binding of $cTnI_{146-158}$ to cNTnC is associated with formation of a rigid alpha-helix comprising cTnI residues 150-158 **[6, 8]**.

When we added $cTnI_{135-209}$ to filamentous F-actin, all NMR signals broadened out beyond detection, consistent with a molecular tumbling rate too slow to allow the use of solution NMR spectroscopy. We, therefore, added DNase I to actin to maintain it in a monomeric form, with the total molecular weight of the complex ~74 kDa. Addition of a 10% molar ratio of actin-DNase I to $cTnI_{135-209}$ caused sequence-specific broadening of $cTnI_{135-209}$ **(Figure 3A)**, indicating that the kinetics of $cTnI_{135-209}$ binding to actin-DNase I occur within the fast exchange regime with respect to the NMR signal frequency differences between free and bound states. (If binding were in the slow exchange regime, binding of a 1:10 ratio actin-DNase I to $cTnI_{135-209}$ could at most obliterate 10% of the signal.) The degree of signal attenuation provides a rough estimate of which regions of $cTnI_{135-209}$ acquire the greatest structural changes upon interacting with actin-DNase I. More tightly bound residues will experience a greater degree of signal broadening caused by the relatively slow tumbling of the ternary complex, whereas this effect is reduced by rapid internal motions in less restricted residues. Signal broadening additionally occurs due to conformational exchange between free and actin-bound $cTnI_{135-209}$ states. In the fast exchange regime, the residues that broaden most will be those that most frequently occupy bound states and those with the largest chemical shift differences between free and bound states (thus moving towards an intermediate exchange regime). In any case, the regions of $cTnI_{135-209}$ that broaden most are those that experience the largest structural dynamic changes upon interaction with actin.

In the 2D ^{1}H-^{15}N spectrum of $cTnI_{135-209}$ in the absence of actin-DNase I, the inhibitory region, residues 135-147, contain weak signals that became undetectable upon addition of actin-DNase I, confirming that the region interacts with actin, as expected **(Figure 3A)**. A small peptide consisting of only cTnI residues 136-147 alone is capable of completely inhibiting actin-myosin cross-bridging, demonstrating this to be the minimal actin-binding inhibitory region **[51]**. Residues 147-177, which includes the switch region, broaden considerably upon addition of

actin-DNase I, suggesting substantial structuring upon binding to actin-DNase I. This finding is consistent with the work of Tripet *et al*. (1997), which showed a "second actin-binding region" within a region corresponding to cTnI residues 164-180. In summary, our data indicate that residues 135-177, comprising the inhibitory region, switch region, and second actin-binding region, acquires rigid structure upon interaction with actin-DNase I.

The rest of the C-terminal tail of cTnI, residues 178-209, appears to be more loosely tethered to actin-DNase I than residues 135-177 **(Figure 3B)**. However, the helical C-terminal region from residues 190-198 appears to be more tightly bound than adjacent segments. This is consistent with the study of Ramos (1999) [52], which found that the last 17 residues of chicken skeletal troponin I (corresponding to residues 193-209 in the current construct) also contribute to a third actin-interacting region in cTnI.

It is noteworthy that the regions of $cTnI_{135-209}$ that experience the largest structural changes upon binding actin-DNase I are the same regions found to possess alpha-helical propensity (**Figure 3B**), with the exception of the inhibitory region $cTnI_{135-147}$. It is therefore quite possible that the same regions acquire additional helical structure when bound to actin. In contrast, residues 178-192 and 201-209 have negligible intrinsic helical propensity and do not appear to broaden as much upon binding actin, which suggests that the folded "mobile domain" detected by Murakami et al. **[50]** could be formed by cTnI residues 135-177, rather than 164-209, as originally proposed. Nevertheless, it is important to note that all residues in $cTnI_{135-209}$ broaden upon binding actin-DNase I, including the less structured regions, which may represent flexible loops that bind to actin through predominantly electrostatic interactions. In fact, mutations associated with hypertrophic or restrictive cardiomyopathy are found throughout the sequence of $cTnI_{135-209}$ **[53]**, suggesting that residues along its entire length are important to interactions with the actin thin filament.

In vitro proteolysis of cTnI by MMP-2 and calpain-2

Proteolytic cleavage of purified recombinant human cardiac troponin constructs, $cTnI_{1-77}$ and $cTnI_{135-209}$, was monitored by SDS-PAGE **(Supplementary Figure 1)**. $cTnI_{1-77}$ runs as a single 16 kDa band, which is higher than its actual (mass spectrometry-confirmed) weight of 8.6 kDa, likely due to its high proportion of positively charged residues. $cTnI_{135-209}$ similarly runs slower than predicted on SDS-PAGE. $cTnI_{1-77}$ and $cTnI_{135-209}$ were readily proteolysed by MMP-2, and this was almost entirely abolished by the MMP inhibitor, ARP-100 **(Supplementary Figure 1A, 1B)**. Similarly, calpain-2 readily cleaved $cTnI_{1-77}$ and $cTnI_{135-209}$, and this was blocked by the calpain inhibitor, MDL-28710. **(Supplementary Figure 1C, 1D)**.

Mass spectrometric identification of MMP-2 cleavage sites of cTnI

Reversed-phase high-performance liquid chromatography-mass spectrometry was used to identify MMP-2-derived cleavage sites in $cTnI_{1-77}$ and $cTnI_{135-209}$. We observed cleavage products after incubation with MMP-2 for 10 min, 30 min, 2 h, 6 h and 24 h **(see Supplementary files and Figure 5)**. At 0 min, intact $cTnI_{1-77}$ appeared at its expected molecular weight, 8627 Da. Within 10 min of incubation, cleavage products were formed corresponding to $cTnI_{1-17}$ (1663.8 Da) and $cTnI_{18-77}$ (6980.9 Da) **(Figure 4 and Supplementary file 1)**, and these continued to predominate even after 24 h of digestion. Thus, there appears to be a single main cleavage site for MMP-2 within $cTnI_{1-77}$ at ^{12}RPAPAP-IRRRSS^{23}.

MMP-2-mediated cleavage of $cTnI_{135-209}$ occurs at two sites that were apparent after 10 min of digestion: ^{151}DAMMQA-LLGARAK^{163} and ^{194}IDALSG-MEGRKK^{205} **(Supplementary file 1).** The cleavage site at A156-L157 is preferred, because it is entirely cleaved at 2 h, whereas the more C-terminal site at G199-M200 is not entirely cleaved, even after 24 h. (Note that $cTnI_{135-209}$ was ^{15}N-labeled for NMR studies, so its molecular mass was increased by the amount expected from replacing the naturally occurring ^{14}N isotope with ^{15}N).

The MMP-2 cleavage sites identified within $cTnI_{1-77}$ and $cTnI_{135-209}$ are consistent with computer-aided prediction of MMP-2 cleavage sites http://cleavpredict.sanfordburnham.org/ **[54]** and consensus sequences derived from MMP-2-catalyzed cleavage of peptide libraries **[55-57]**, which show a strong preference for a hydrophobic residue (particularly leucine, isoleucine, methionine) in the P1' site (the residue immediately C-terminal to the cleavage site), as well as a proline or hydrophobic β-branched residue (valine or isoleucine) at P3 (the third residue N-terminal to the cleavage site). A feature that is somewhat unique to MMP-2 is its predilection for small amino acid residues like glycine, alanine, or serine at positions P2, P1, and P3'.

Mass spectrometric identification of calpain-2 cleavage sites of cTnI

We also mapped calpain-2 specific cleavage sites within $cTnI_{1-77}$ and $cTnI_{135-209}$ using mass spectrometry **(Supplementary file 2)**. We identified calpain-2-mediated $cTnI_{1-77}$ and $cTnI_{135-209}$ cleavage products after 0 min, 10 min, 2 h, 6 h and 24 h (**See supplementary files 2 and 3)**. At 0 min, intact $cTnI_{1-77}$ is observed at its expected molecular weight 8627 Da (**See supplementary file 2)**, though cleavage products have already appeared, with the most prominent fragments being $cTnI_{1-28}$ (3088 Da), $cTnI_{1-29}$ (3159 Da), $cTnI_{29-77}$ (5557 Da), $cTnI_{30-77}$ (5486 Da), and $cTnI_{50-77}$ (3225 Da), suggesting rapid proteolysis even before the reaction is immediately stopped by adding 1% v/v formic acid and the reaction vial frozen in liquid nitrogen. Thus, calpain-2-mediated proteolysis of cTnI occurs at a much faster rate than that observed with MMP-2. By 10 min (see **Supplementary file 2**), intermediate cleavage products like $cTnI_{1-49}$ (5419.9 Da) and $cTnI_{30-77}$ (5486.1 Da) are disappearing, while smaller cleavage fragments begin to predominate: $cTnI_{1-25}$ (2697.4 Da), $cTnI_{1-28}$ (3087.6 Da), $cTnI_{1-29}$ (3158.6 Da), $cTnI_{27-49}$ (2583 Da), $cTnI_{26-49}$ (2739.6 Da), $cTnI_{50-77}$ (3224.8 Da), and $cTnI_{53-77}$ (2897.6 Da). These terminal products are still present after 24

h, suggesting that the major cleavage sites for calpain are all clustered around cTnI residues 25-30 and 49-53.

For calpain-2 digestion of $cTnI_{135-209}$, we identified intact ^{15}N labelled $cTnI_{135-209}$ with expected molecular weight 8964.4 Da at 0 min **(See supplementary file 3)**. Similar to $cTnI_{1-77}$, the major cleavage products of $cTnI_{135-209}$ can also be detected from 0 min. After 10 min incubation, numerous major cleavage sites are apparent. Strikingly the calpain-2 activity localizes predominantly to the hydrophobic switch region, with a total of 6 different sites located between residues 152 and 160 (**Figure 5**). This is consistent with the known sequence preferences of calpains-1 and -2. Of note is the cleavage site at ^{156}ALL-GAR^{161}, which has a striking similarity to the optimal calpain cleavage sequence PLF-AAR determined by peptide library analysis **[58]** and alanine scanning mutagenesis **[30]**, with hydrophobic residues on either side of the central scissile bond. Additional calpain cleavage sites are located N-terminal to residues R145, A170, and Q174.

In contrast to the very specific cut sites of MMP-2, calpain-2 appears to possess much broader substrate specificity, having multiple cleavage sites within $cTnI_{1-77}$ and $cTnI_{135-209}$ **(Figure 5)**. Remarkably, calpain cut sites occur in all cTnI segments that are involved in protein-protein interactions. It seems as though calpain targets protein regions above a certain threshold of hydrophobicity, and these tend to be the same segments involved in protein-protein interactions: $cTnI_{25-30}$ contains four calpain cleavage sites and is the most hydrophobic segment of $cTnI_{19-37}$, which interacts with cNTnC; $cTnI_{49-53}$ contains three calpain cleavage sites and is the most hydrophobic segment of $cTnI_{39-60}$, which forms an alpha helix that binds tightly to cCTnC; and $cTnI_{152-160}$ contains six calpain cleavage sites and includes the most hydrophobic segment of the cTnI switch region, $cTnI_{146-158}$. Full activation of calpain would have a devastating effect on cardiac troponin I function, severely disabling calcium-mediated excitation-contraction coupling. However, it is necessary to determine which physiologic protein-protein interactions protect cTnI from proteolysis, as detailed in the sections below.

In vitro proteolysis of $cTnI_{1-77}$ in the presence of cTnC

We examined proteolysis of $cTnI_{1-77}$ in the presence of its only known binding partner, cTnC. $cTnI_{1-77}$ interacts with both globular domains of cTnC in two distinct ways. cTnI residues 39-60 bind tightly to the C-terminal domain of cTnC (cCTnC) as a well-structured alpha-helix that extends down to residue 79 **[8]**. In contrast, $cTnI_{1-37}$ is intrinsically disordered, with $cTnI_{19-37}$ interacting with the cNTnC domain through predominantly electrostatic interactions **[39]**.

cTnC binding had virtually no effect on MMP-2-mediated digestion of $cTnI_{1-77}$ **(Supplementary Figure 2A)**, which occurs between residues 17 and 18 **(Figure 5)**. This cut site lies just N-terminal to $cTnI_{19-37}$, which interacts with cNTnC **[39]**. Calpain-2-mediated digestion

of $cTnI_{1-77}$ yields two partially digested intermediate fragments at 11 and 12 kDa on SDS-PAGE corresponding roughly to fragments $cTnI_{30-77}$ and $cTnI_{1-49}$, respectively. Upon addition of cTnC, the larger fragment corresponding to residues 1-49 disappears completely **(Supplementary Figure 2B)**, which makes sense because the cut sites between residues 49 and 53 lie exactly in the middle of the alpha helix (cTnI residues 39-60) that binds very tightly to cCTnC. Thus, formation of a rigid alpha helix precludes calpain-mediated proteolysis at this site in its native biologic context. In contrast, when $cTnI_{19-37}$ binds electrostatically to the cTnC N-terminal domain, cTnI residues 25-31 display a partial restriction in mobility, but retain an intrinsically disordered random coil state **[39]**. Apparently this interaction provides only partial protection from calpain-mediated proteolysis, as suggested by **Supplementary Figure 2B** (that is, digestion at this site still produces a prominent 11 kDa band in the presence of cTnC).

Based on earlier biophysical studies, proteolytic removal of the first 17 residues of cTnI by MMP-2 would be expected to slightly decrease the calcium sensitivity of the troponin complex, but not to the same extent as the physiologic phosphorylation of Ser22 and Ser23 **[59]**. Hence, while cTnI is vulnerable to MMP-2 digestion at residues 17-18 when in complex with cTnC, proteolytic cleavage at this site would not be expected to have a devastating impact on cardiac function. In contrast, cleavage at cTnI residues 25-30 by calpain would remove more of the N-terminal tail and have a much larger calcium desensitizing effect **[59]**.

In vitro proteolysis of $cTnI_{135-209}$ in the presence of cTnC

Note that MMP-2 has only two cut sites (between residues 156-157 and 199-200) in $cTnI_{135-209,}$ leading to the production of five different degradation products, producing a surprisingly complex appearance on the SDS-PAGE gels for so few cut sites (Supplementary Figure 1). cTnC binding to $cTnI_{135-209}$ resulted in proteolytic protection against MMP-2 (**Figure 6A**) primarily at the cut site between residues 156 and 157. This results from the binding of the switch region, $cTnI_{146-158}$, to cNTnC, with an alpha helix extending from residues 150-159 **[8]**. In contrast, the C-terminal cut site between cTnI residues 199 and 200, which is not known to form any interaction with cTnC, remains exposed to MMP-2 cleavage. Thus, in the presence of cTnC, this C-terminal locus becomes the preferred MMP-2 cut site in $cTnI_{135-209}$.

Binding of $cTnI_{135-209}$ to cTnC significantly changes its proteolysis pattern by calpain (**Figure 6B**). In the absence of cTnC, the most favoured cut sites are distributed throughout the switch region, between residues 152 and 160, yielding a fragment at about 11 kDa ($cTnI_{153-209}$) on the SDS-PAGE gel and a smaller fragment that runs at the bottom ($cTnI_{135-152}$). However, binding of the $cTnI_{146-158}$ switch region to cNTnC shields it from cleavage, making the cut sites flanking the switch region more probable.

Cleavage of the switch region would be expected to have a devastating effect on cardiac function, making it impossible to activate cardiac muscle contraction. However, it is apparent that binding of $cTnI_{135-209}$ to cTnC specifically protects the switch region against proteolytic digestion, though adjacent segments are still susceptible to calpain-mediated proteolysis.

***In vitro* proteolysis of $cTnI_{135-209}$ in the presence of actin**

We next examined the proteolysis of $cTnI_{135-209}$ in the presence of actin. The current NMR study of $cTnI_{135-209}$ suggests a partial structuring throughout its entire length upon interaction with actin. Incubation of $cTnI_{135-209}$ with actin showed pronounced concentration-dependent inhibition of MMP-2 proteolytic activity, almost completely inhibiting cTnI proteolysis at the highest concentration of actin studied, at a molar ratio of $cTnI_{135-209}$ to actin of 1:1 **(Figure 7A)**. However, even at this concentration of actin, some residual proteolysis at both MMP-2 cut sites is still evident.

Calpain-2-mediated digestion of $cTnI_{135-209}$ in the presence of actin at a 1:1 molar ratio showed partial proteolytic protection of all cut sites, leading to significant preservation of intact $cTnI_{135-209}$ (**Figure 7B**). The degradation band at 11 kDa, corresponding to cleavage of the switch region, remains prominent in the presence of actin. This suggests that actin binding does not protect the switch region to the same extent as binding to cTnC.

It should be noted that within the sarcomere, the stoichiometry of cTnI:actin is 1:7. However, this is the result of a single troponin complex being associated with a single tropomyosin coiled-coil that lies along seven actin monomers. Presumably, in the absence of tropomyosin, the binding site for cTnI is limited to a single actin monomer. The protection of $cTnI_{135-209}$ by a 1:1 molar ratio of actin is suggestive of a 1:1 stoichiometry of binding, as expected.

Discussion

Our study demonstrates that the C-terminal tail of cTnI contains three regions with intrinsic helical propensity, corresponding to the critical switch region that binds to cNTnC, the "second actin binding region" **[60]**, and the "third actin binding region" **[52]**. We further show that all of these regions exhibit structural changes in the presence of actin, and it would not be unreasonable to postulate that they acquire more helical character. Finally, we demonstrate that the C-terminal tail is susceptible to cleavage by MMP-2 and calpain-2, two intracellular proteases that are activated in ischemia-reperfusion injury **[14, 19, 28, 33, 35]**.

Numerous studies in different animal model systems have attempted to address the issue of cTnI proteolysis in ischemia-reperfusion injury **[12, 14, 31, 61-66]**. A fundamental question is which proteases are activated, and at what degree of ischemic injury. One can envision a full spectrum of ischemia-reperfusion injury ranging from immediate recovery of function to

irreversible cell death. Even with cell death, there is a spectrum of functional impairment ranging from ventricular wall akinesis to aneurysm to wall rupture. Central to the understanding of structural damage is the activation of intracellular proteases, of which MMP-2, calpains, and caspases have been identified as major players. (Caspase was found to not digest cTnI in an earlier study **[67]**).

"Myocardial stunning" is a form of reversible injury **[68]** in which restoration of blood flow relieves ischemia, but the viable, post-ischemic myocardium does not recover full contractile function immediately, sometimes requiring hours to days for full restoration **[69, 70]**. The exact mechanism behind stunning remains a mystery, though the stunned cardiomyocyte is believed to be structurally and metabolically intact **[15, 71]**. Most investigations have indicated that calcium handling is unperturbed, but there is decreased maximum force generation and either decreased or unchanged calcium sensitivity **[72-76]**.

Proteolytic digestion of cTnI has previously been proposed as an explanation for myocardial stunning. Past studies focused on a 17-residue C-terminal truncation of cTnI, $cTnI_{1\text{-}193}$, that was associated with decreased Ca^{2+} sensitivity and myocardial stunning **[77]**. Separate biochemical analyses of this cleavage product demonstrated increased, rather than decreased, Ca^{2+} sensitivity **[77, 78]**. We found no evidence to suggest that $cTnI_{1\text{-}193}$ is generated by either MMP-2- or calpain cleavage. On the other hand, we have determined that within the C-terminal tail of cTnI, the critical switch region is most susceptible to cleavage, both by MMP-2 and calpain**,** and cleavage at this site would provide the simplest possible explanation for the phenomenon of myocardial stunning.

The cTnI switch region is partially protected from proteolytic cleavage as it cycles between cNTnC and actin to control cardiac contraction, although severe myocardial ischemia creates additional factors that could release it from both: 1) formation of the actomyosin "rigor" state due to depletion of ATP [79]; and 2) intracellular acidosis causing calcium desensitization of the cNTnC domain. (It should be noted that acidosis would also compromise the calcium-dependent activity of calpains, however.) The necessary convergence of multiple factors under sub-lethal conditions is a possible explanation for why myocardial stunning is not universally observed in all experimental and clinical settings involving ischemia-reperfusion injury.

The proteolytic cleavage of cTnI residues C-terminal to the switch region would likely also have a negative impact on cardiac function. The importance of C-terminal residues is underscored by the existence of many hypertrophic cardiomyopathy-associated mutations that extend all the way to E208 **[53]**. A recent case study of a 30-year-old man with progressive heart failure associated with restrictive cardiomyopathy identified a 15-residue (D195-S209) deletion from the C-terminus of cTnI **[80]**.

There is a complex interplay between cTnI proteolysis, phosphorylation, cardiomyopathy-associated mutations, and different disease states. The most consistently observed phosphorylation site in humans is at cTnI S22 and S23, which modulates the calcium sensitivity of cardiac muscle [4, 5]. The phosphorylation state of cTnI S22/S23 is impacted by the presence of heart failure [81] or cardiomyopathy-related mutations [82, 83]. Phosphorylation at S22 and S23 by protein kinase A [84] or just S23 by protein kinase D [85] has also been shown to decrease calpain-mediated proteolysis. Phosphorylation at this site may interfere with calpain-mediated proteolysis at Y25-R26 or R26-A27.

More recently, phosphorylation of S198 by protein kinase C has been shown to increase the calcium sensitivity cardiac muscle [86]. Further studies in transgenic mice found that the pseudophosphorylation mutation S198D decreased formation of a proteolyzed form of cTnI following 30 min of global ischemia and 1 h of reperfusion **[62]**. An S198A mutation did not attenuate proteolytic digestion. The simplest explanation is that the cTnI S198D mutation abolishes the MMP-2 cleavage site at G199-M200, whereas the S198A mutation does not, as suggested by MMP-2 cleavage site amino acid preferences at position P2 **[55]**.

Proteolytic digestion of cTnI during myocardial ischemia has clinical consequences beyond impairment of cardiac function. Proteolytic cleavage results in the generation of heterogeneous fragments of cTnI that are released into the bloodstream and used in the detection and diagnosis of myocardial infarction **[87, 88]**. In a recently published study, we demonstrate that the degree of proteolysis in cTnI depends on the severity of ischemic injury, with the highest degree of digestion observed in patients with ST-elevation myocardial infarct and lesser degrees of digestion seen in supply-demand ischemia **[89]**. It is thus quite possible that the pattern of cTnI proteolysis could be used to differentiate between different mechanisms of myocardial injury.

In summary, cardiac troponin I contains intrinsically disordered tails that are key to its function but are also sensitive to proteolysis by the proteases purported to be active during ischemia-reperfusion injury. Proteolytic digestion of cTnI has important implications for cardiac muscle function, as well as for the clinical diagnosis of myocardial infarction via the detection of cTnI fragments.

Acknowledgements

The authors would like to acknowledge helpful discussions with Dr. John Dawson (University of Guelph) regarding cardiac actin. This work was supported by start-up funds from the Faculty of Medicine and Dentistry and Department of Medicine and the Hwang Professional Corporation

to P.H. and Canadian Institutes of Health Research (CIHR) Foundation grants to R.S. and P.L.D. P.H. is supported by a Phase 2 Clinician-Scientist Salary Award from CIHR and an Emerging Research Leadership Initiative grant from the Mazankowski Alberta Heart Institute and Heart and Stroke Foundation of Canada.

Author contributions:

Zabed Mahmud: Conceptualization; Data curation; Formal analysis; Methodology; Writing-original draft. Somaya Zahran: Conceptualization; Data curation; Formal analysis; Investigation; Methodology; Writing-original draft; Equal contribution. Philip Liu: Resources; Methodology. Bela Reiz: Resources; Data curation. Brandon Chan: Methodology. Andrej Roczkowsky: Methodology. Christian-Scott McCartney: Methodology. Peter Davies: Resources; Writing-review and editing. Liang Li: Resources; Writing-review and editing. Richard Schulz: Conceptualization; Resources; Supervision; Funding acquisition; Validation; Writing-review and editing. Peter Hwang: Conceptualization; Resources; Formal analysis; Supervision; Funding acquisition; Investigation; Writing-original draft.

Conflict of interest

The authors declare that they have no conflicts of interest related to the contents of this article.

References

[1] S. Ebashi, F. Ebashi, A new protein factor promoting contraction of actomyosin, Nature, 203 (1964) 645-646.
[2] S. Ebashi, F. Ebashi, A. Kodama, Troponin as the Ca++-receptive protein in the contractile system, J Biochem, 62 (1967) 137-138.
[3] M.L. Greaser, J. Gergely, Purification and properties of the components from troponin, J Biol Chem, 248 (1973) 2125-2133.
[4] B.J. Biesiadecki, K. Tachampa, C. Yuan, J.P. Jin, P.P. de Tombe, R.J. Solaro, Removal of the cardiac troponin I N-terminal extension improves cardiac function in aged mice, J Biol Chem, 285 (2010) 19688-19698.
[5] J. Wattanapermpool, X. Guo, R.J. Solaro, The unique amino-terminal peptide of cardiac troponin I regulates myofibrillar activity only when it is phosphorylated, J Mol Cell Cardiol, 27 (1995) 1383-1391.
[6] M.X. Li, L. Spyracopoulos, B.D. Sykes, Binding of cardiac troponin-I147-163 induces a structural opening in human cardiac troponin-C, Biochemistry, 38 (1999) 8289-8298.
[7] F. Cai, M.X. Li, S.E. Pineda-Sanabria, S. Gelozia, S. Lindert, F. West, B.D. Sykes, P.M. Hwang, Structures reveal details of small molecule binding to cardiac troponin, J Mol Cell Cardiol, 101 (2016) 134-144.
[8] S. Takeda, A. Yamashita, K. Maeda, Y. Maeda, Structure of the core domain of human cardiac troponin in the Ca(2+)-saturated form, Nature, 424 (2003) 35-41.

[9] M.J. Suskiewicz, J.L. Sussman, I. Silman, Y. Shaul, Context-dependent resistance to proteolysis of intrinsically disordered proteins, Protein Sci, 20 (2011) 1285-1297.
[10] Z. Liu, Y. Huang, Advantages of proteins being disordered, Protein Sci, 23 (2014) 539-550.
[11] I.A. Katrukha, A.E. Kogan, A.V. Vylegzhanina, A.V. Kharitonov, N.N. Tamm, V.L. Filatov, A.V. Bereznikova, E.V. Koshkina, A.G. Katrukha, Full-size cardiac troponin I and tts proteolytic fragments in blood of patients with acute myocardial infarction: antibody selection for assay development, Clin Chem, 64 (2018) 1104-1112.
[12] J.L. McDonough, D.K. Arrell, J.E. Van Eyk, Troponin I degradation and covalent complex formation accompanies myocardial ischemia/reperfusion injury, Circ Res, 84 (1999) 9-20.
[13] R.J. Solaro, Troponin I, stunning, hypertrophy, and failure of the heart, Circ Res, 84 (1999) 122-124.
[14] W. Wang, C.J. Schulze, W.L. Suarez-Pinzon, J.R. Dyck, G. Sawicki, R. Schulz, Intracellular action of matrix metalloproteinase-2 accounts for acute myocardial ischemia and reperfusion injury, Circulation, 106 (2002) 1543-1549.
[15] R. Bolli, E. Marban, Molecular and cellular mechanisms of myocardial stunning, Physiol Rev, 79 (1999) 609-634.
[16] P. Ferdinandy, R. Schulz, Nitric oxide, superoxide, and peroxynitrite in myocardial ischaemia-reperfusion injury and preconditioning, Br J Pharmacol, 138 (2003) 532-543.
[17] M. Miyamae, S.A. Camacho, M.W. Weiner, V.M. Figueredo, Attenuation of postischemic reperfusion injury is related to prevention of $[Ca^{2+}]$m overload in rat hearts, Am J Physiol, 271 (1996) H2145-2153.
[18] E. Marban, M. Kitakaze, H. Kusuoka, J.K. Porterfield, D.T. Yue, V.P. Chacko, Intracellular free calcium concentration measured with 19F NMR spectroscopy in intact ferret hearts, Proc Natl Acad Sci U S A, 84 (1987) 6005-6009.
[19] B.G. Hughes, R. Schulz, Targeting MMP-2 to treat ischemic heart injury, Basic Res Cardiol, 109 (2014) 424.
[20] S. Viappiani, A.C. Nicolescu, A. Holt, G. Sawicki, B.D. Crawford, H. Leon, T. van Mulligen, R. Schulz, Activation and modulation of 72kDa matrix metalloproteinase-2 by peroxynitrite and glutathione, Biochem Pharmacol, 77 (2009) 826-834.
[21] R. Bolli, B.S. Patel, M.O. Jeroudi, E.K. Lai, P.B. McCay, Demonstration of free radical generation in "stunned" myocardium of intact dogs with the use of the spin trap alpha-phenyl N-tert-butyl nitrone, J Clin Invest, 82 (1988) 476-485.
[22] R.S. Vander Heide, C. Steenbergen, Cardioprotection and myocardial reperfusion: pitfalls to clinical application, Circ Res, 113 (2013) 464-477.
[23] W. Yasmin, K.D. Strynadka, R. Schulz, Generation of peroxynitrite contributes to ischemia-reperfusion injury in isolated rat hearts, Cardiovasc Res, 33 (1997) 422-432.
[24] S.J. Franco, A. Huttenlocher, Regulating cell migration: calpains make the cut, J Cell Sci, 118 (2005) 3829-3838.
[25] M.C. Lebart, Y. Benyamin, Calpain involvement in the remodeling of cytoskeletal anchorage complexes, FEBS J, 273 (2006) 3415-3426.
[26] B. Siegmund, Y.V. Ladilov, H.M. Piper, Importance of sodium for recovery of calcium control in reoxygenated cardiomyocytes, Am J Physiol, 267 (1994) H506-513.
[27] D.E. Goll, V.F. Thompson, H. Li, W. Wei, J. Cong, The calpain system, Physiol Rev, 83 (2003) 731-801.
[28] M. Neri, I. Riezzo, N. Pascale, C. Pomara, E. Turillazzi, Ischemia/reperfusion injury following acute myocardial infarction: a critical issue for clinicians and forensic pathologists, Mediators Inflamm, 2017 (2017) 7018393.
[29] C.E. McCartney, J.A. MacLeod, P.A. Greer, P.L. Davies, An easy-to-use FRET protein substrate to detect calpain cleavage in vitro and in vivo, Biochim Biophys Acta, 1865 (2018) 221-230.
[30] J.C. Kelly, D. Cuerrier, L.A. Graham, R.L. Campbell, P.L. Davies, Profiling of calpain activity with a series of FRET-based substrates, Biochim Biophys Acta, 1794 (2009) 1505-1509.

[31] A. Maekawa, J.K. Lee, T. Nagaya, K. Kamiya, K. Yasui, M. Horiba, K. Miwa, M. Uzzaman, M. Maki, Y. Ueda, I. Kodama, Overexpression of calpastatin by gene transfer prevents troponin I degradation and ameliorates contractile dysfunction in rat hearts subjected to ischemia/reperfusion, J Mol Cell Cardiol, 35 (2003) 1277-1284.
[32] P.Y. Cheung, G. Sawicki, M. Wozniak, W. Wang, M.W. Radomski, R. Schulz, Matrix metalloproteinase-2 contributes to ischemia-reperfusion injury in the heart, Circulation, 101 (2000) 1833-1839.
[33] J. Inserte, V. Hernando, D. Garcia-Dorado, Contribution of calpains to myocardial ischaemia/reperfusion injury, Cardiovasc Res, 96 (2012) 23-31.
[34] K. Yoshida, M. Inui, K. Harada, T.C. Saido, Y. Sorimachi, T. Ishihara, S. Kawashima, K. Sobue, Reperfusion of rat heart after brief ischemia induces proteolysis of calspectin (nonerythroid spectrin or fodrin) by calpain, Circ Res, 77 (1995) 603-610.
[35] M. Chen, D.J. Won, S. Krajewski, R.A. Gottlieb, Calpain and mitochondria in ischemia/reperfusion injury, J Biol Chem, 277 (2002) 29181-29186.
[36] A.G. Katrukha, A.V. Bereznikova, V.L. Filatov, T.V. Esakova, O.V. Kolosova, K. Pettersson, T. Lovgren, T.V. Bulargina, I.R. Trifonov, N.A. Gratsiansky, K. Pulkki, L.M. Voipio-Pulkki, N.B. Gusev, Degradation of cardiac troponin I: implication for reliable immunodetection, Clin Chem, 44 (1998) 2433-2440.
[37] P.M. Hwang, J.S. Pan, B.D. Sykes, A PagP fusion protein system for the expression of intrinsically disordered proteins in Escherichia coli, Protein Expr Purif, 85 (2012) 148-151.
[38] S. Zahran, J.S. Pan, P.B. Liu, P.M. Hwang, Combining a PagP fusion protein system with nickel ion-catalyzed cleavage to produce intrinsically disordered proteins in E. coli, Protein Expr Purif, 116 (2015) 133-138.
[39] P.M. Hwang, F. Cai, S.E. Pineda-Sanabria, D.C. Corson, B.D. Sykes, The cardiac-specific N-terminal region of troponin I positions the regulatory domain of troponin C, Proc Natl Acad Sci U S A, 111 (2014) 14412-14417.
[40] F. Delaglio, S. Grzesiek, G.W. Vuister, G. Zhu, J. Pfeifer, A. Bax, NMRPipe: a multidimensional spectral processing system based on UNIX pipes, J Biomol NMR, 6 (1995) 277-293.
[41] B.A. Johnson, Using NMRView to visualize and analyze the NMR spectra of macromolecules, Methods Mol Biol, 278 (2004) 313-352.
[42] A. De Simone, A. Cavalli, S.T. Hsu, W. Vranken, M. Vendruscolo, Accurate random coil chemical shifts from an analysis of loop regions in native states of proteins, J Am Chem Soc, 131 (2009) 16332-16333.
[43] C. Camilloni, A. De Simone, W.F. Vranken, M. Vendruscolo, Determination of secondary structure populations in disordered states of proteins using nuclear magnetic resonance chemical shifts, Biochemistry, 51 (2012) 2224-2231.
[44] W. Kabsch, H.G. Mannherz, D. Suck, E.F. Pai, K.C. Holmes, Atomic structure of the actin:DNase I complex, Nature, 347 (1990) 37-44.
[45] S. Baghirova, B.G. Hughes, M. Poirier, M.Y. Kondo, R. Schulz, Nuclear matrix metalloproteinase-2 in the cardiomyocyte and the ischemic-reperfused heart, J Mol Cell Cardiol, 94 (2016) 153-161.
[46] J.S. Elce, C. Hegadorn, S. Gauthier, J.W. Vince, P.L. Davies, Recombinant calpain II: improved expression systems and production of a C105A active-site mutant for crystallography, Protein Eng, 8 (1995) 843-848.
[47] P. Sheterline, J. Clayton, J. Sparrow, Actin, Protein Profile, 2 (1995) 1-103.
[48] E. Gasteiger, A. Gattiker, C. Hoogland, I. Ivanyi, R.D. Appel, A. Bairoch, ExPASy: The proteomics server for in-depth protein knowledge and analysis, Nucleic Acids Res, 31 (2003) 3784-3788.
[49] T.M. Blumenschein, D.B. Stone, R.J. Fletterick, R.A. Mendelson, B.D. Sykes, Dynamics of the C-terminal region of TnI in the troponin complex in solution, Biophys J, 90 (2006) 2436-2444.
[50] K. Murakami, F. Yumoto, S.Y. Ohki, T. Yasunaga, M. Tanokura, T. Wakabayashi, Structural basis for Ca2+-regulated muscle relaxation at interaction sites of troponin with actin and tropomyosin, J Mol Biol, 352 (2005) 178-201.

[51] J.E. Van Eyk, L.T. Thomas, B. Tripet, R.J. Wiesner, J.R. Pearlstone, C.S. Farah, F.C. Reinach, R.S. Hodges, Distinct regions of troponin I regulate Ca2+-dependent activation and Ca2+ sensitivity of the acto-S1-TM ATPase activity of the thin filament, J Biol Chem, 272 (1997) 10529-10537.
[52] C.H. Ramos, Mapping subdomains in the C-terminal region of troponin I involved in its binding to troponin C and to thin filament, J Biol Chem, 274 (1999) 18189-18195.
[53] J. Mogensen, T. Hey, S. Lambrecht, A systematic review of phenotypic features associated with cardiac troponin I mutations in hereditary cardiomyopathies, Can J Cardiol, 31 (2015) 1377-1385.
[54] S. Kumar, B.I. Ratnikov, M.D. Kazanov, J.W. Smith, P. Cieplak, CleavPredict: a platform for reasoning about matrix metalloproteinases proteolytic events, PLoS One, 10 (2015) e0127877.
[55] U. Eckhard, P.F. Huesgen, O. Schilling, C.L. Bellac, G.S. Butler, J.H. Cox, A. Dufour, V. Goebeler, R. Kappelhoff, U. Auf dem Keller, T. Klein, P.F. Lange, G. Marino, C.J. Morrison, A. Prudova, D. Rodriguez, A.E. Starr, Y. Wang, C.M. Overall, Active site specificity profiling datasets of matrix metalloproteinases (MMPs) 1, 2, 3, 7, 8, 9, 12, 13 and 14, Data Brief, 7 (2016) 299-310.
[56] U. Eckhard, P.F. Huesgen, O. Schilling, C.L. Bellac, G.S. Butler, J.H. Cox, A. Dufour, V. Goebeler, R. Kappelhoff, U.A. Keller, T. Klein, P.F. Lange, G. Marino, C.J. Morrison, A. Prudova, D. Rodriguez, A.E. Starr, Y. Wang, C.M. Overall, Active site specificity profiling of the matrix metalloproteinase family: Proteomic identification of 4300 cleavage sites by nine MMPs explored with structural and synthetic peptide cleavage analyses, Matrix Biol, 49 (2016) 37-60.
[57] B.E. Turk, L.L. Huang, E.T. Piro, L.C. Cantley, Determination of protease cleavage site motifs using mixture-based oriented peptide libraries, Nat Biotechnol, 19 (2001) 661-667.
[58] D. Cuerrier, T. Moldoveanu, P.L. Davies, Determination of peptide substrate specificity for mu-calpain by a peptide library-based approach: the importance of primed side interactions, J Biol Chem, 280 (2005) 40632-40641.
[59] D.G. Ward, M.P. Cornes, I.P. Trayer, Structural consequences of cardiac troponin I phosphorylation, J Biol Chem, 277 (2002) 41795-41801.
[60] B. Tripet, J.E. Van Eyk, R.S. Hodges, Mapping of a second actin-tropomyosin and a second troponin C binding site within the C terminus of troponin I, and their importance in the Ca2+-dependent regulation of muscle contraction, J Mol Biol, 271 (1997) 728-750.
[61] W.D. Gao, D. Atar, Y. Liu, N.G. Perez, A.M. Murphy, E. Marban, Role of troponin I proteolysis in the pathogenesis of stunned myocardium, Circ Res, 80 (1997) 393-399.
[62] Y. Li, G. Zhu, N. Paolocci, P. Zhang, C. Takahashi, N. Okumus, A. Heravi, G. Keceli, G. Ramirez-Correa, D.A. Kass, A.M. Murphy, Heart failure-related hyperphosphorylation in the cardiac troponin I C terminus has divergent effects on cardiac function in vivo, Circ Heart Fail, 10 (2017).
[63] D.A. Colantonio, J.E. Van Eyk, K. Przyklenk, Stunned peri-infarct canine myocardium is characterized by degradation of troponin T, not troponin I, Cardiovasc Res, 63 (2004) 217-225.
[64] S.J. Kim, R.K. Kudej, A. Yatani, Y.K. Kim, G. Takagi, R. Honda, D.A. Colantonio, J.E. Van Eyk, D.E. Vatner, R.L. Rasmusson, S.F. Vatner, A novel mechanism for myocardial stunning involving impaired Ca(2+) handling, Circ Res, 89 (2001) 831-837.
[65] S.M. Schwartz, J.Y. Duffy, J. Pearl, S. Goins, C.J. Wagner, D.P. Nelson, Glucocorticoids preserve calpastatin and troponin I during cardiopulmonary bypass in immature pigs, Pediatr Res, 54 (2003) 91-97.
[66] A.M. Murphy, H. Kogler, D. Georgakopoulos, J.L. McDonough, D.A. Kass, J.E. Van Eyk, E. Marban, Transgenic mouse model of stunned myocardium, Science, 287 (2000) 488-491.
[67] C. Communal, M. Sumandea, P. de Tombe, J. Narula, R.J. Solaro, R.J. Hajjar, Functional consequences of caspase activation in cardiac myocytes, Proc Natl Acad Sci U S A, 99 (2002) 6252-6256.
[68] F.R. Eberli, Stunned myocardium--an unfinished puzzle, Cardiovasc Res, 63 (2004) 189-191.
[69] G.R. Heyndrickx, R.W. Millard, R.J. McRitchie, P.R. Maroko, S.F. Vatner, Regional myocardial functional and electrophysiological alterations after brief coronary artery occlusion in conscious dogs, J Clin Invest, 56 (1975) 978-985.

[70] R. Bolli, W.X. Zhu, J.I. Thornby, P.G. O'Neill, R. Roberts, Time course and determinants of recovery of function after reversible ischemia in conscious dogs, Am J Physiol, 254 (1988) H102-114.
[71] G. Heusch, R. Schulz, Characterization of hibernating and stunned myocardium, Eur Heart J, 18 Suppl D (1997) D102-110.
[72] T. Ehring, R. Schulz, G. Heusch, Characterization of "hibernating" and "stunned" myocardium with focus on the use of calcium antagonists in "stunned" myocardium, J Cardiovasc Pharmacol, 20 Suppl 5 (1992) S25-33.
[73] W.D. Gao, D. Atar, P.H. Backx, E. Marban, Relationship between intracellular calcium and contractile force in stunned myocardium. Direct evidence for decreased myofilament Ca2+ responsiveness and altered diastolic function in intact ventricular muscle, Circ Res, 76 (1995) 1036-1048.
[74] W.D. Gao, Y. Liu, R. Mellgren, E. Marban, Intrinsic myofilament alterations underlying the decreased contractility of stunned myocardium. A consequence of Ca2+-dependent proteolysis?, Circ Res, 78 (1996) 455-465.
[75] K.S. McDonald, R.L. Moss, W.P. Miller, Incorporation of the troponin regulatory complex of post-ischemic stunned porcine myocardium reduces myofilament calcium sensitivity in rabbit psoas skeletal muscle fibers, J Mol Cell Cardiol, 30 (1998) 285-296.
[76] J.E. Van Eyk, F. Powers, W. Law, C. Larue, R.S. Hodges, R.J. Solaro, Breakdown and release of myofilament proteins during ischemia and ischemia/reperfusion in rat hearts: identification of degradation products and effects on the pCa-force relation, Circ Res, 82 (1998) 261-271.
[77] D.B. Foster, T. Noguchi, P. VanBuren, A.M. Murphy, J.E. Van Eyk, C-terminal truncation of cardiac troponin I causes divergent effects on ATPase and force: implications for the pathophysiology of myocardial stunning, Circ Res, 93 (2003) 917-924.
[78] H.M. Rarick, X.H. Tu, R.J. Solaro, A.F. Martin, The C terminus of cardiac troponin I is essential for full inhibitory activity and Ca2+ sensitivity of rat myofibrils, J Biol Chem, 272 (1997) 26887-26892.
[79] J.P. Davis, C. Norman, T. Kobayashi, R.J. Solaro, D.R. Swartz, S.B. Tikunova, Effects of thin and thick filament proteins on calcium binding and exchange with cardiac troponin C, Biophys J, 92 (2007) 3195-3206.
[80] S. Shah, H. Yogasundaram, R. Basu, F. Wang, D.I. Paterson, T.P. Alastalo, G.Y. Oudit, Novel dominant-negative mutation in cardiac troponin I causes severe restrictive cardiomyopathy, Circ Heart Fail, 10 (2017).
[81] N. Hamdani, W.J. Paulus, L. van Heerebeek, A. Borbely, N.M. Boontje, M.J. Zuidwijk, J.G. Bronzwaer, W.S. Simonides, H.W. Niessen, G.J. Stienen, J. van der Velden, Distinct myocardial effects of beta-blocker therapy in heart failure with normal and reduced left ventricular ejection fraction, Eur Heart J, 30 (2009) 1863-1872.
[82] V. Sequeira, P.J. Wijnker, L.L. Nijenkamp, D.W. Kuster, A. Najafi, E.R. Witjas-Paalberends, J.A. Regan, N. Boontje, F.J. Ten Cate, T. Germans, L. Carrier, S. Sadayappan, M.A. van Slegtenhorst, R. Zaremba, D.B. Foster, A.M. Murphy, C. Poggesi, C. Dos Remedios, G.J. Stienen, C.Y. Ho, M. Michels, J. van der Velden, Perturbed length-dependent activation in human hypertrophic cardiomyopathy with missense sarcomeric gene mutations, Circ Res, 112 (2013) 1491-1505.
[83] A.V. Gomes, K. Harada, J.D. Potter, A mutation in the N-terminus of troponin I that is associated with hypertrophic cardiomyopathy affects the Ca(2+)-sensitivity, phosphorylation kinetics and proteolytic susceptibility of troponin, J Mol Cell Cardiol, 39 (2005) 754-765.
[84] F. Di Lisa, R. De Tullio, F. Salamino, R. Barbato, E. Melloni, N. Siliprandi, S. Schiaffino, S. Pontremoli, Specific degradation of troponin T and I by mu-calpain and its modulation by substrate phosphorylation, Biochem J, 308 (Pt 1) (1995) 57-61.
[85] A. Martin-Garrido, B.J. Biesiadecki, H.E. Salhi, Y. Shaifta, C.G. Dos Remedios, S. Ayaz-Guner, W. Cai, Y. Ge, M. Avkiran, J.C. Kentish, Monophosphorylation of cardiac troponin-I at Ser-23/24 is sufficient to

regulate cardiac myofibrillar Ca(2+) sensitivity and calpain-induced proteolysis, J Biol Chem, 293 (2018) 8588-8599.
[86] P.J. Wijnker, Y. Li, P. Zhang, D.B. Foster, C. dos Remedios, J.E. Van Eyk, G.J. Stienen, A.M. Murphy, J. van der Velden, A novel phosphorylation site, Serine 199, in the C-terminus of cardiac troponin I regulates calcium sensitivity and susceptibility to calpain-induced proteolysis, J Mol Cell Cardiol, 82 (2015) 93-103.
[87] K. Thygesen, J.S. Alpert, A.S. Jaffe, M.L. Simoons, B.R. Chaitman, H.D. White, E.S.C.A.A.H.A.W.H.F.T.F.f.U.D.o.M.I. Joint, C. Authors/Task Force Members, K. Thygesen, J.S. Alpert, H.D. White, S. Biomarker, A.S. Jaffe, H.A. Katus, F.S. Apple, B. Lindahl, D.A. Morrow, E.C.G. Subcommittee, B.R. Chaitman, P.M. Clemmensen, P. Johanson, H. Hod, S. Imaging, R. Underwood, J.J. Bax, J.J. Bonow, F. Pinto, R.J. Gibbons, S. Classification, K.A. Fox, D. Atar, L.K. Newby, M. Galvani, C.W. Hamm, S. Intervention, B.F. Uretsky, P.G. Steg, W. Wijns, J.P. Bassand, P. Menasche, J. Ravkilde, Trials, S. Registries, E.M. Ohman, E.M. Antman, L.C. Wallentin, P.W. Armstrong, M.L. Simoons, Trials, S. Registries, J.L. Januzzi, M.S. Nieminen, M. Gheorghiade, G. Filippatos, Trials, S. Registries, R.V. Luepker, S.P. Fortmann, W.D. Rosamond, D. Levy, D. Wood, Trials, S. Registries, S.C. Smith, D. Hu, J.L. Lopez-Sendon, R.M. Robertson, D. Weaver, M. Tendera, A.A. Bove, A.N. Parkhomenko, E.J. Vasilieva, S. Mendis, E.S.C.C.f.P. Guidelines, J.J. Bax, H. Baumgartner, C. Ceconi, V. Dean, C. Deaton, R. Fagard, C. Funck-Brentano, D. Hasdai, A. Hoes, P. Kirchhof, J. Knuuti, P. Kolh, T. McDonagh, C. Moulin, B.A. Popescu, Z. Reiner, U. Sechtem, P.A. Sirnes, M. Tendera, A. Torbicki, A. Vahanian, S. Windecker, R. Document, J. Morais, C. Aguiar, W. Almahmeed, D.O. Arnar, F. Barili, K.D. Bloch, A.F. Bolger, H.E. Botker, B. Bozkurt, R. Bugiardini, C. Cannon, J. de Lemos, F.R. Eberli, E. Escobar, M. Hlatky, S. James, K.B. Kern, D.J. Moliterno, C. Mueller, A.N. Neskovic, B.M. Pieske, S.P. Schulman, R.F. Storey, K.A. Taubert, P. Vranckx, D.R. Wagner, Third universal definition of myocardial infarction, J Am Coll Cardiol, 60 (2012) 1581-1598.
[88] L. Babuin, A.S. Jaffe, Troponin: the biomarker of choice for the detection of cardiac injury, CMAJ, 173 (2005) 1191-1202.
[89] S. Zahran, Figueiredo,V.P., Graham, M.M., Schulz,R., Hwang, P.M, Proteolytic digestion of serum cardiac troponin I a marker of ischemic severity, Journal Applied Lab Med, (2018) *In press*.

Figure legends

Figure 1

Calcium-saturated cardiac troponin complex. Cardiac troponin C (cTnC) is shown in blue and consists of an N-terminal domain (cNTnC) and a C-terminal domain (cCTnC). Troponin I (cTnI) is shown in magenta and red, with the red regions corresponding to the two constructs used in this study: $cTnI_{1\text{-}77}$ and $cTnI_{135\text{-}209}$. The inset highlights the N- and C-terminal tails of cTnI, with intrinsically disordered drawn manually as squiggles. Figure prepared using PyMOL and structure 4Y99 (PDB code). At resting calcium concentrations, cNTnC releases calcium (yellow sphere), adopts a closed conformation, and $cTnI_{135\text{-}209}$ binds to actin. The bar diagram at the bottom shows domain organization and different functional regions of cTnI with its binding partners. Note that our numbering of cTnI excludes the N-terminal methionine, which is removed and replaced by an acetyl group during post-translational processing.

Figure 2

(A) Residue-specific secondary structure of $cTnI_{135\text{-}209}$ calculated by the program δ2D using backbone NMR chemical shifts. The functional regions shown highlight the results of limited binding studies in the past, rather than exact boundaries determined from structure. **(B)** Summary of medium-range NOE connectivities $d_{\alpha\beta\ (i,\ i+3)}$ that are specific for alpha-helical structure. **(C)** Representative strip plots showing helical medium-range NOEs from 3D ^{15}N- edited NOESY-HSQC and 3D ^{13}C edited NOESY-HSQC.

Figure 3

2D [^{1}H, ^{15}N]-HSQC NMR spectra of $cTnI_{135\text{-}209}$. **(A)** $cTnI_{135\text{-}209}$ without actin-DNase I (left) or with actin-DNase I (right). The insets show the ^{15}N-upfield region of the spectrum containing, Gly, Ser, and Thr residues. Addition of a small amount of monomeric actin-DNase I complex into $cTnI_{135\text{-}209}$ causes differential signal broadening (right). Residues belonging to the inhibitory region (green), switch region (red), and second actin binding region (blue) become undetectable upon addition of actin-DNase I **(B)** The observed reduction in signal intensities in the 2D [^{1}H, ^{15}N]-HSQC signals of $cTnI_{135\text{-}209}$ when actin-DNase I complex is added. Overlapped signals or signals with weak intensity were excluded.

Figure 4

Mass spectrometry data of cTnI [1-77] proteolysed by MMP-2 at 10 min incubation time point. Proteolysed fragments of cTnI [1-77] were eluted at different retention times, and the molecular weights of fragments were determined by reverse phase high performance liquid chromatography followed by mass spectrometry.

Figure 5

Summary of mass spectrometric analysis identifying MMP-2 and calpain-2 cleavage sites within $cTnI_{1-77}$ and $cTnI_{135-209}$ (included in Supplementary Data).

Figure 6

Comparison of *in vitro* proteolysis of $cTnI_{135-209}$ in the presence or absence of cTnC by MMP-2 **(A)** and calpain-2 (**B**) in representative Coomassie blue-stained SDS–PAGE gel (N=3). Cardiac troponin C is not susceptible to either MMP-2 or calpain-2 proteolysis and appears intact as a single band at ~21 KDa**.** 2 µg of cTnI was loaded in every reaction lane. Molar cTnI-to-cTnC ratio was 1 to 1. The incubation period was 2 h at 37 °C.

Figure 7

Comparison of in vitro proteolysis of $cTnI_{135-209}$ in the presence or absence of actin by MMP-2 and calpain-2 in representative Coomassie Blue-stained SDS–PAGE gels (N=3). Molar actin:cTnI ratios are indicated above the gel. Incubation duration was 2 h at 37°C. 2 µg of cTnI was loaded in every reaction lane. MMP-2-to-cTnI ratio was 1:500, and calpain-2-to-cTnI ratio was 1:250.

Online supplemental material

Supplementary figure 1: Representative Coomassie blue-stained 16% Tris-Tricine gels illustrating *in vitro* proteolysis of $cTnI_{1-77}$ or $cTnI_{135-209}$ by proteases MMP-2 or calpain-2 (N=3). Molar protease-to-substrate are shown above each gel. 2 µg of cTnI was loaded in every reaction lane. Incubations were 2 h at 37 °C. Inhibition of MMP-2 and calpain-2 activities by ARP-100 and MDL-28710, respectively, is also shown.

Supplementary figure 2: Comparison of *in vitro* proteolysis of $cTnI_{1-77}$ in the presence or absence of cTnC by MMP-2 **(A)** and calpain-2 (**B**) in representative Coomassie blue-stained SDS–PAGE gel (N=3). Cardiac troponin C is not susceptible to either MMP-2 or calpain-2 proteolysis and appears

intact as a single band at ~21 KDa**.** 2 µg of cTnI was loaded in every reaction lane. Molar cTnI-to-cTnC ratio was 1 to 1. The incubation period was 2 h at 37 °C.

Supplementary file 1: Mass spectrometry data of cTnI [1-77] and cTnI [135-209] proteolysed by MMP-2 at time points from 0 min to 24 h.

Supplementary file 2: Mass spectrometry data of cTnI [1-77] proteolysed by calpain-2 at time points from 0 min to 24 h.

Supplementary file 3 Mass spectrometry data of cTnI [135-209] proteolysed by calpain-2 at time points from 0 min to 24 h.

Figure 1

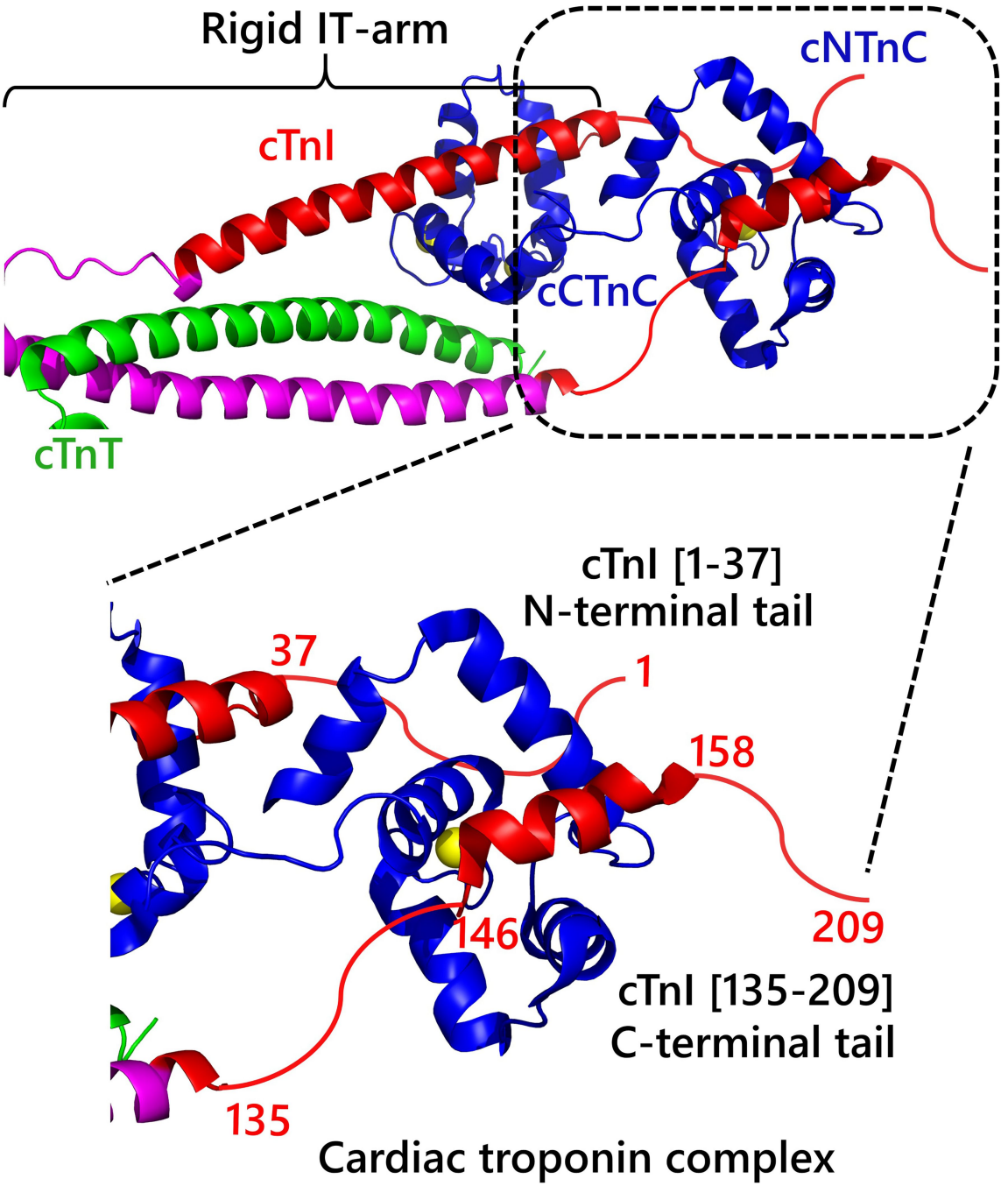

Cardiac troponin complex

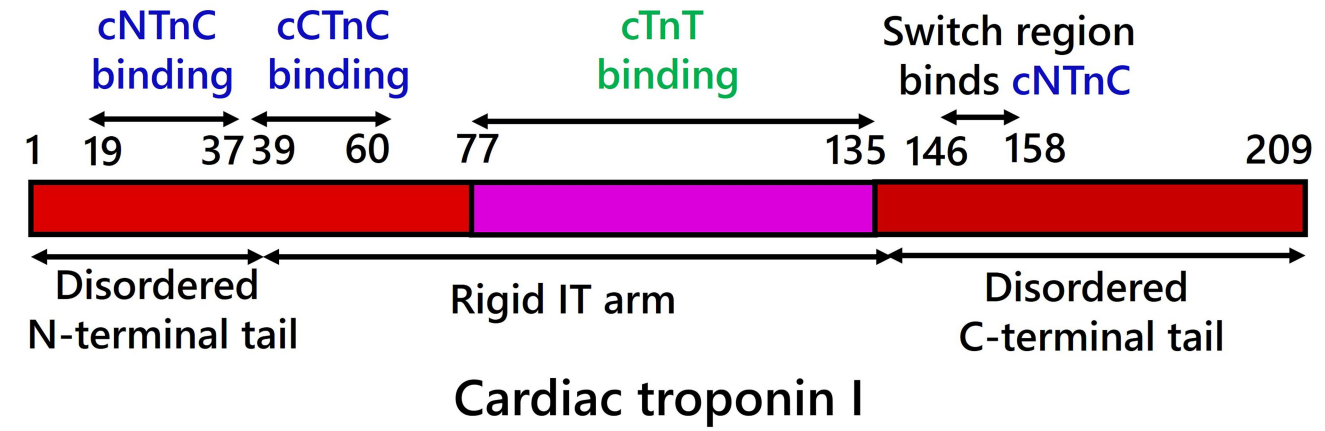

Cardiac troponin I

Figure 2

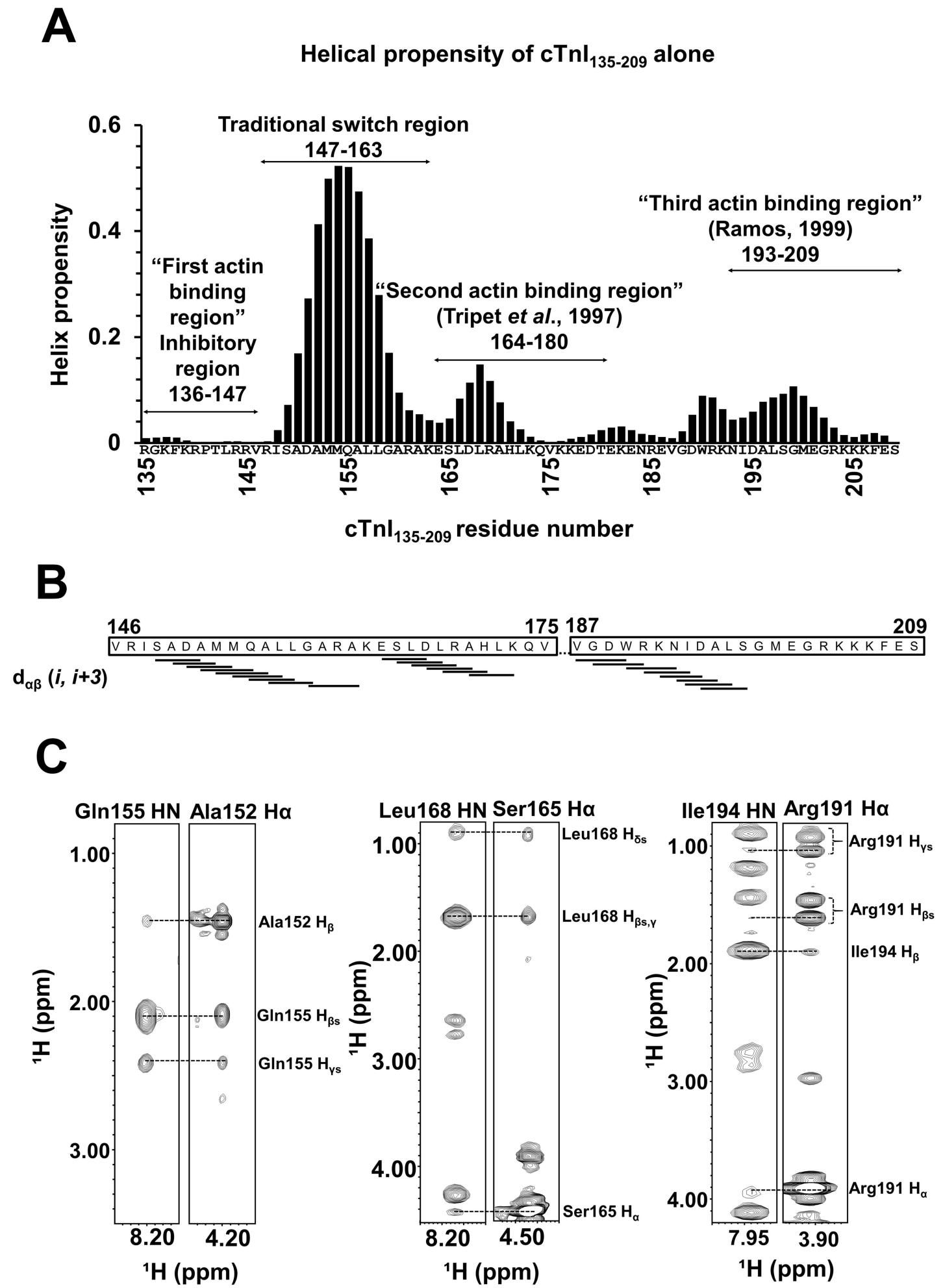
A
Helical propensity of cTnI135-209 alone
Traditional switch region
147-163
"First actin binding region" Inhibitory region 136-147
"Second actin binding region" (Tripet et al., 1997) 164-180
"Third actin binding region" (Ramos, 1999) 193-209
Helix propensity
0.6
0.4
0.2
0
RGKFKRPTLRRVRISADAMMQALLGARAKESLDLRAHLKQVKKEDTEKENREVGDWRKNIDALSGMEGRKKKFES
135
145
155
165
175
185
195
205
cTnI135-209 residue number
B
146
175
187
209
V R I S A D A M M Q A L L G A R A K E S L D L R A H L K Q V
V G D W R K N I D A L S G M E G R K K K F E S
dαβ (i, i+3)
C
Gln155 HN
Ala152 Hα
Ala152 Hβ
Gln155 Hβs
Gln155 Hγs
1.00
2.00
3.00
1H (ppm)
8.20
4.20
1H (ppm)
Leu168 HN
Ser165 Hα
Leu168 Hδs
Leu168 Hβs,γ
Ser165 Hα
1.00
2.00
3.00
4.00
1H (ppm)
8.20
4.50
1H (ppm)
Ile194 HN
Arg191 Hα
Arg191 Hγs
Arg191 Hβs
Ile194 Hβ
Arg191 Hα
1.00
2.00
3.00
4.00
1H (ppm)
7.95
3.90
1H (ppm)

Figure 3

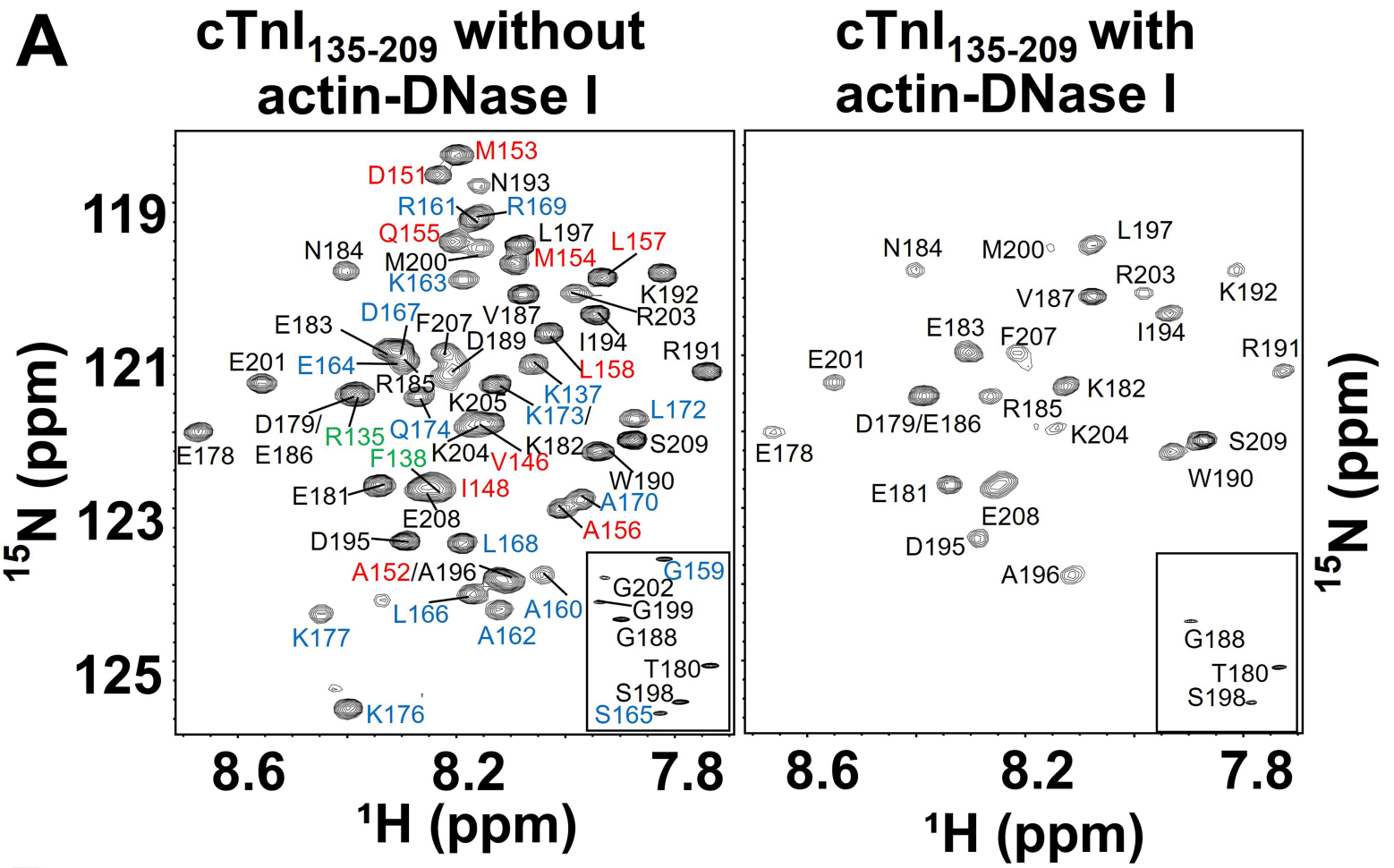
A
cTnI135-209 without actin-DNase I
cTnI135-209 with actin-DNase I
15N (ppm)
1H (ppm)
119
121
123
125
8.6
8.2
7.8
M153
D151
N193
R161
R169
Q155
L197
L157
N184
M200
M154
K163
K192
D167
F207
V187
R203
E183
D189
I194
R191
E201
E164
L158
R185
K205
K137
D179/
K173/
L172
R135
Q174
S209
E178
E186
F138
K204
V146
K182
W190
E181
I148
A170
E208
A156
D195
L168
A152/A196
G159
G202
L166
A160
G199
K177
A162
G188
T180
S198
S165
K176
N184
M200
L197
R203
K192
V187
E183
F207
I194
R191
E201
K182
D179/E186
R185
K204
S209
E178
W190
E181
E208
D195
A196
G188
T180
S198

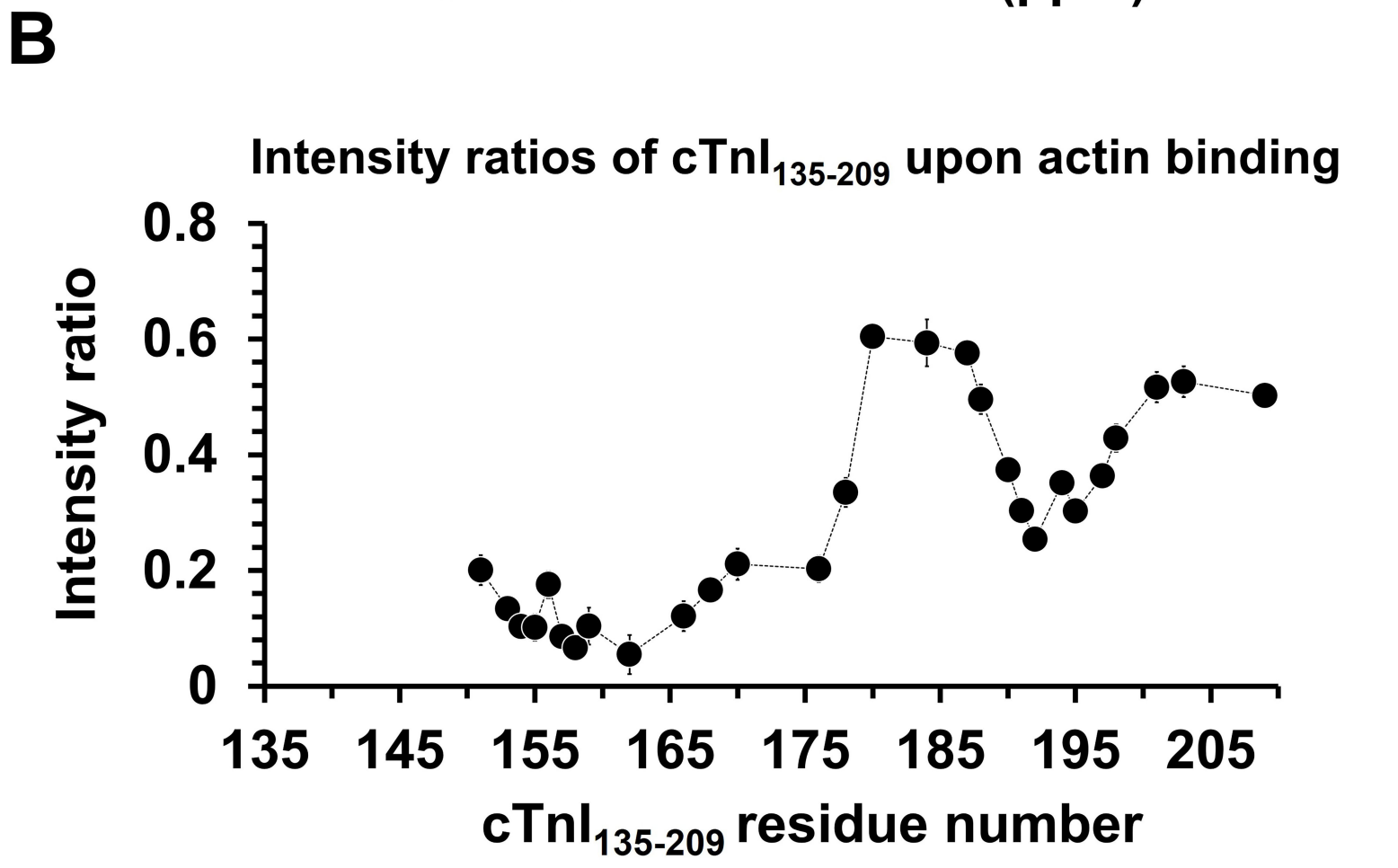
B
Intensity ratios of cTnI135-209 upon actin binding
Intensity ratio
0.8
0.6
0.4
0.2
0
135
145
155
165
175
185
195
205
cTnI135-209 residue number

Figure 4

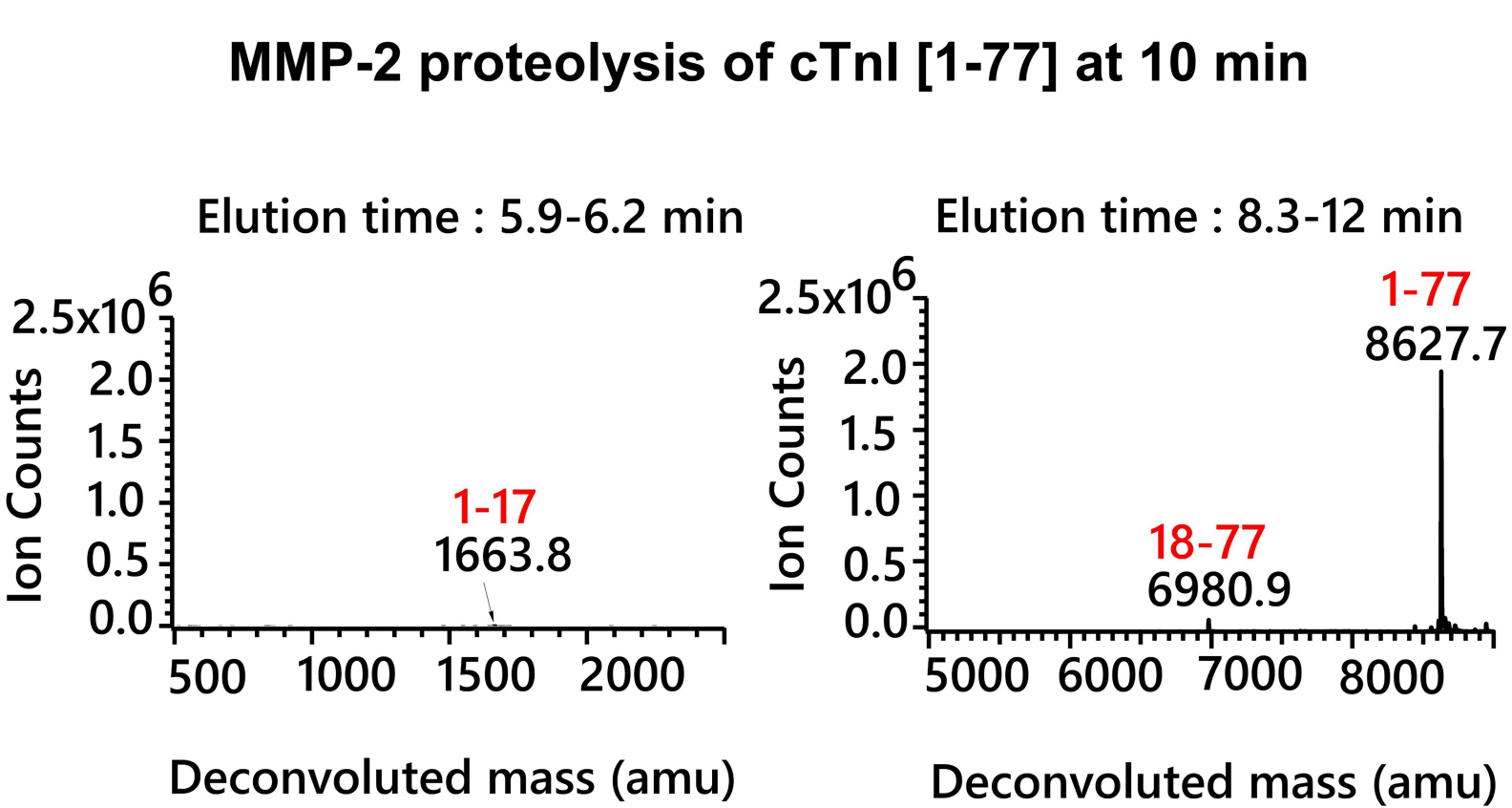
MMP-2 proteolysis of cTnI [1-77] at 10 min
Elution time : 5.9-6.2 min
2.5x10^6
2.0
1.5
1.0
0.5
0.0
Ion Counts
1-17
1663.8
500
1000
1500
2000
Deconvoluted mass (amu)
Elution time : 8.3-12 min
2.5x10^6
2.0
1.5
1.0
0.5
0.0
Ion Counts
1-77
8627.7
18-77
6980.9
5000
6000
7000
8000
Deconvoluted mass (amu)

Figure 5

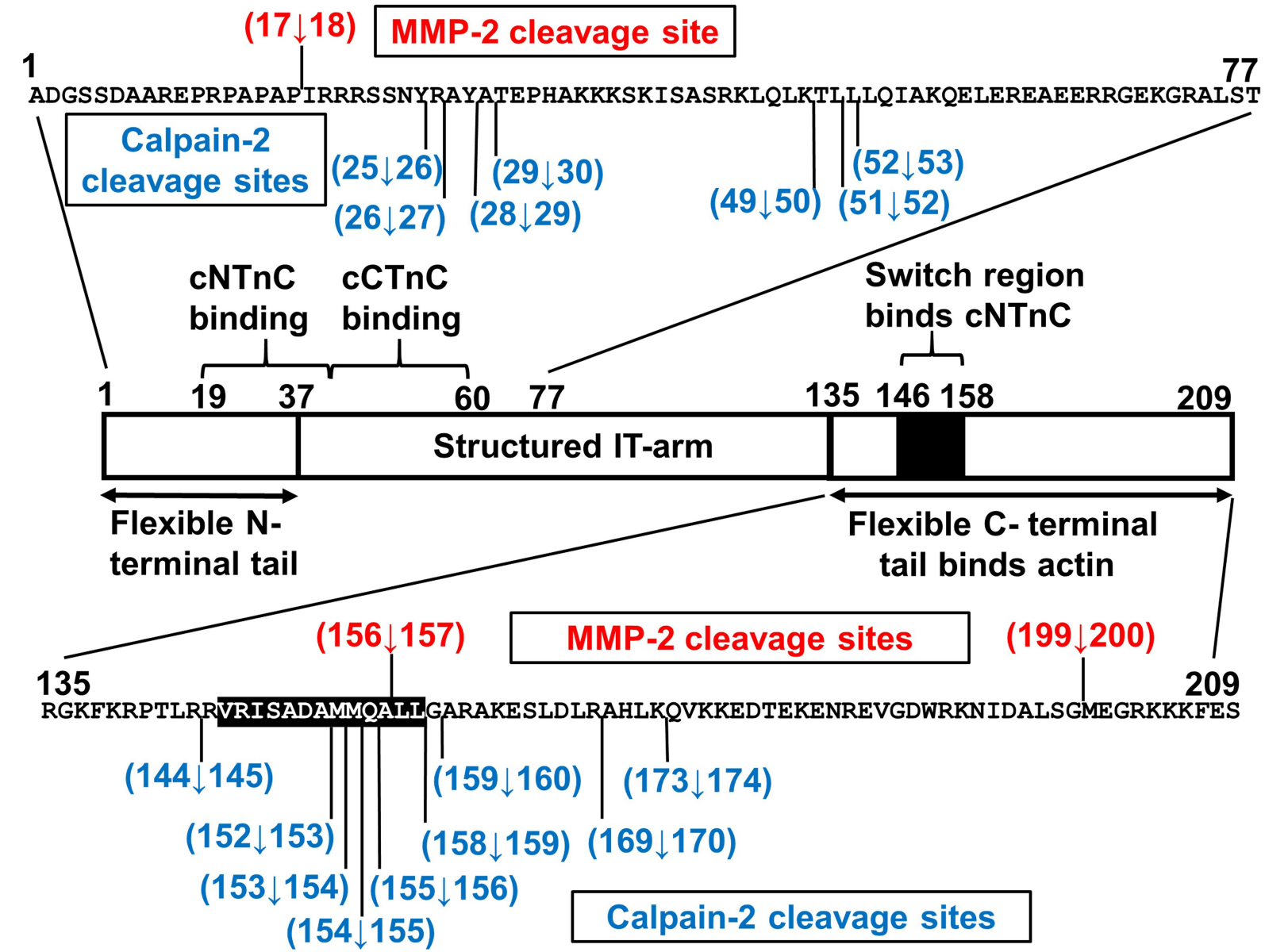
(17↓18)
MMP-2 cleavage site
1
77
ADGSSDAAREPRPAPAPIRRRSSNYRAYATEPHAKKKSKISASRKLQLKTLLLQIAKQELEREAEERRGEKGRALST
Calpain-2 cleavage sites
(25↓26)
(26↓27)
(29↓30)
(28↓29)
(49↓50)
(51↓52)
(52↓53)
cNTnC binding
cCTnC binding
Switch region binds cNTnC
1
19
37
60
77
135
146
158
209
Structured IT-arm
Flexible N-terminal tail
Flexible C- terminal tail binds actin
(156↓157)
MMP-2 cleavage sites
(199↓200)
135
209
RGKFKRPTLRRVRISADAMMQALLGARAKESLDLRAHLKQVKKEDTEKENREVGDWRKNIDALSGMEGRKKKFES
(144↓145)
(152↓153)
(153↓154)
(154↓155)
(155↓156)
(158↓159)
(159↓160)
(169↓170)
(173↓174)
Calpain-2 cleavage sites

Figure 6

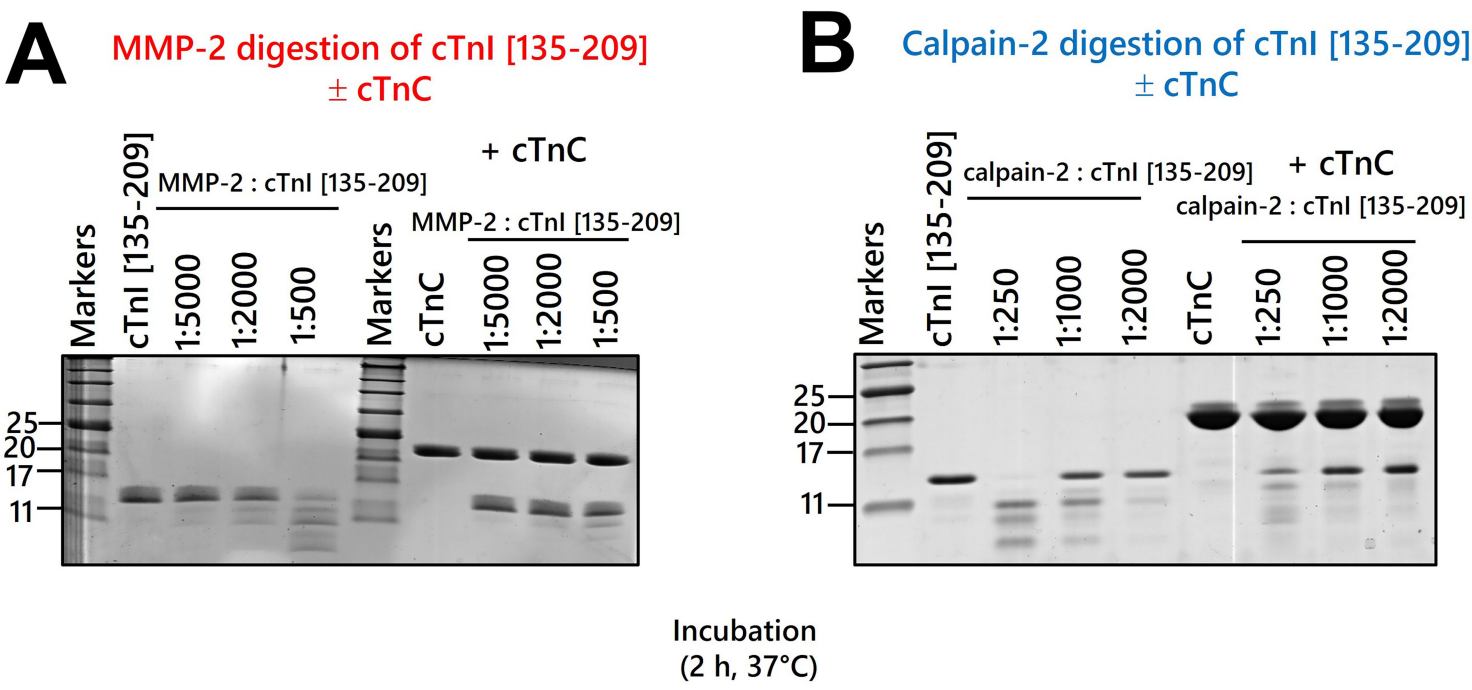
A
MMP-2 digestion of cTnI [135-209]
± cTnC
Markers
cTnI [135-209]
MMP-2 : cTnI [135-209]
1:5000
1:2000
1:500
+ cTnC
MMP-2 : cTnI [135-209]
Markers
cTnC
1:5000
1:2000
1:500
25
20
17
11
B
Calpain-2 digestion of cTnI [135-209]
± cTnC
Markers
cTnI [135-209]
calpain-2 : cTnI [135-209]
1:250
1:1000
1:2000
+ cTnC
calpain-2 : cTnI [135-209]
cTnC
1:250
1:1000
1:2000
25
20
17
11
Incubation
(2 h, 37°C)

Figure 7

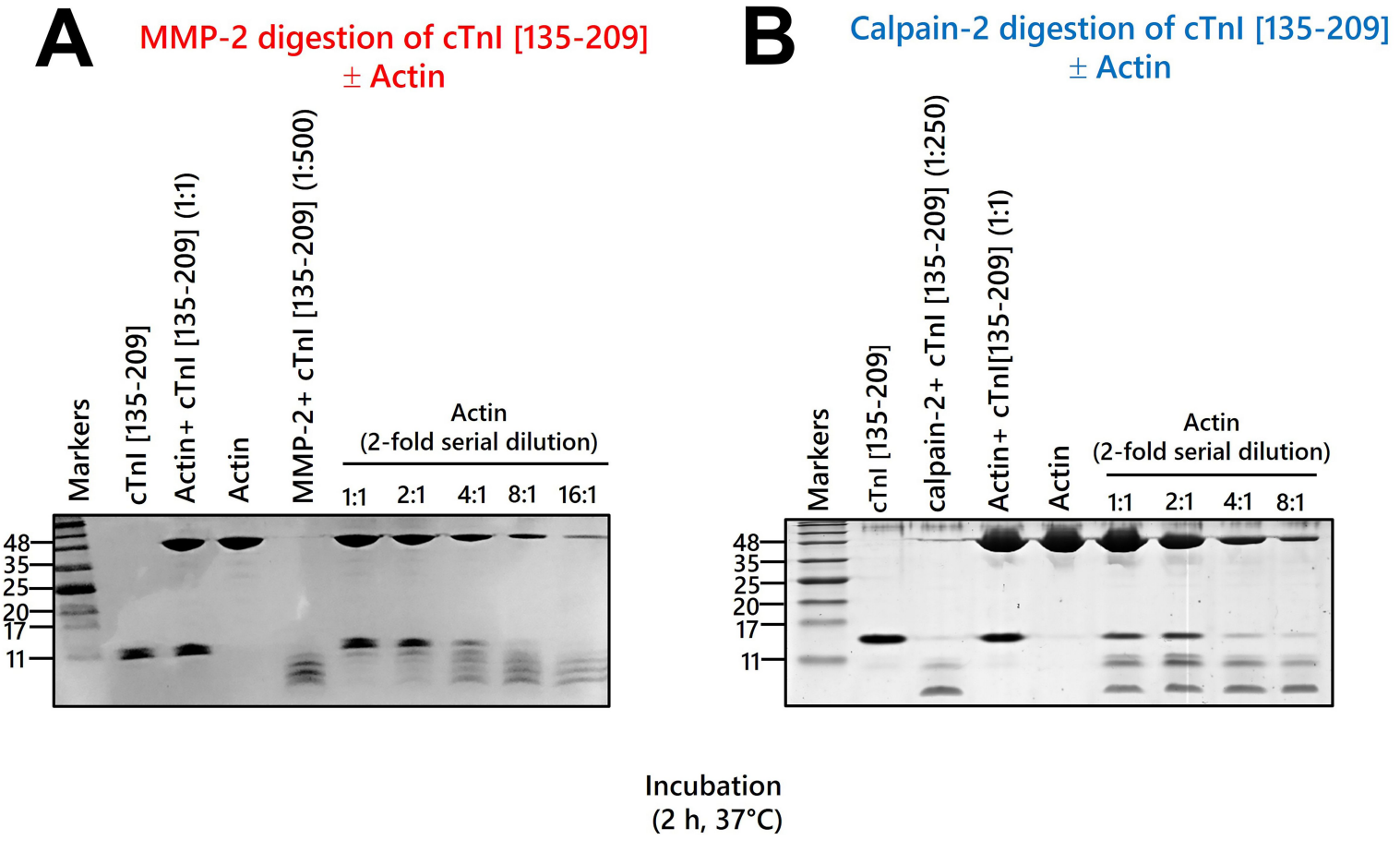
A
MMP-2 digestion of cTnI [135-209]
± Actin
Markers
cTnI [135-209]
Actin+ cTnI [135-209] (1:1)
Actin
MMP-2+ cTnI [135-209] (1:500)
Actin
(2-fold serial dilution)
1:1
2:1
4:1
8:1
16:1
48
35
25
20
17
11
B
Calpain-2 digestion of cTnI [135-209]
± Actin
Markers
cTnI [135-209]
calpain-2+ cTnI [135-209] (1:250)
Actin+ cTnI[135-209] (1:1)
Actin
Actin
(2-fold serial dilution)
1:1
2:1
4:1
8:1
48
35
25
20
17
11
Incubation
(2 h, 37°C)

Supplementary Figure 1

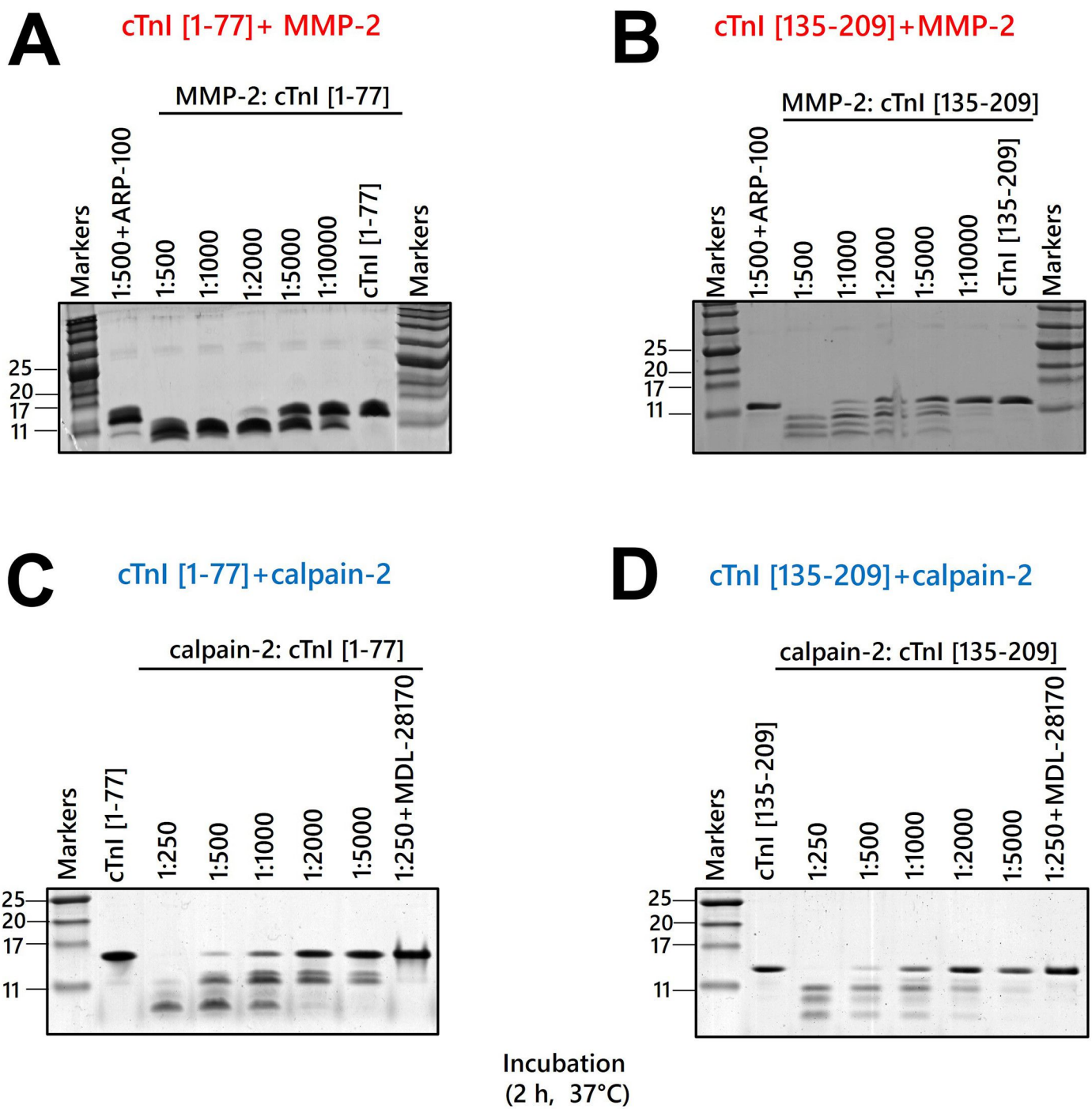

Supplementary Figure 2